STYRELSEN FÖR VINTERSJÖFARTSFORSKNING
Sjöfartsverket Sverige, Sjöfartsstyrelsen Finland
Forskningsrapport nr 16:4

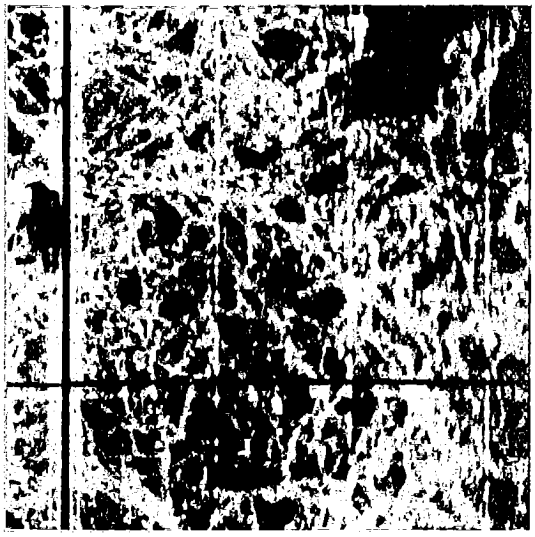

Analysis of SLAR data

by Surendra Parashar

Norrköping 1976

WINTER NAVIGATION RESEARCH BOARD
Swedish Administration of Shipping and Navigation, Finnish Board of Navigation
Research Report No 16:4

Cover picture:
The icebreaker TOR in the middle of the test area for SEA ICE -75 and a SLAR registration.

SMHI
Fack
S-601 01 Norrköping

SEA ICE 75

Analysis of SLAR data

by Surendra Parashar
consultant for SLAR analysis

Norrköping 1976

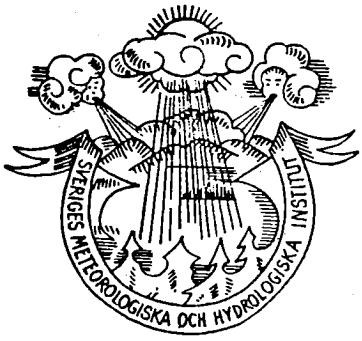

Printed in Sweden
DIREKTOFFSET
Norrköping 1976

Table of Contents

Foreword 4
1. Introduction 5
2. Formation of Sea Ice 7
3. Radar Scattering 9
4. "Sea Ice -75" Experiment 12
5. Ground Truth Information 14
6. SLAR Data 16
7. Preliminary Analysis of SLAR Data 19
8. Recommendations 39
9. Summary of Results 43
10. Conclusions 44
References 45

Foreword

The Winter Navigation Research Board presents report no. 16:4. This report contains a careful analysis of the registrations received from the Side-looking Airborne Radar (SLAR) that for the first time was tested in Sweden in connection with the remote sensing experiment SEA ICE-75. The technical details of the radar and the carrier, together with a description of the operational procedures and results, can be found in report no. 16:3 of these series.

As the SLAR was a new instrument that hade never been tested for ice mapping in Sweden before it was decided that extra care should be taken in analysing the registrations obtained. A SLAR expert from Kansas University in USA, Dr Surendra Parashar, was therefore engaged for a 2 months period to undertake such an analysis. The expenditures for Dr Parashars stay in Sweden were covered by the Swedish Board for Space Activities and office facilities were provided by the Swedish Meteorological and Hydrological Institute (SMHI). This enabled him to work in close collaboration with the staff of the maritime section, responsible for the ground truth programme.

In this report Dr Parashar has not only presented an exellent analysis of the SLAR data, but he has also provided necessary background information for the understanding of the conclusions and recommendations made.

The Winter Navigation Research Board wish to sincerely thank Dr Parashar for his most vauable contribution to the project SEA ICE-75.

Thanks are also extended to the Swedish Board for Space Activities, and to Swedish Meteorological and Hydrological Institute for providing the necessary funds and office facilities.

Norrköping and Helsingfors, July 1976.

Lennart Johansson **Helge Jääsalo**

1 Introduction

The purpose of this report is to present results obtained from the analysis of SLAR (Side-Looking Airborne Radar) data collected during the "Sea Ice -75" experiment. This experiment was conducted in the Bay of Bothnia during March, 1975. The data gathered during this remote sensing experiment included SLAR images of sea ice obtained by utilizing EMI X-band (wavelength, $\lambda \approx 3$ cm) real-aperture radar. Despite the fact that the radar images are of poor to moderate quality, a number of meaningful conclusions can be drawn. On the basis of these results, recommedations are made for the design of future experiments and for the operating parameters that may be used in an operational ice mapping radar system.

In an effort to help explain and understand some of the results, included are sections on the formation of sea ice and its relevant characteristics, the nature of radar return from sea ice, and sea ice parameters of interest. The purpose, objective, and the design of "Sea Ice -75" experiment, with the type of data collected from it, is reported briefly. In addition, a summary of important results and the capability and utility of SLAR in mapping ice is included along with the meaningful conclusions in the end.

To be able to compare the results presented here with past measurements, the following section contains a brief historical background on the use of radar for mapping ice.

1.1 Purpose and Background of Radar Measurement of Ice

Despite the knowledge that sea ice covers a very large area, it has been only recently that attempts have been made to learn more about sea ice. It appears that the environment of the earth's surface is greatly influenced by the sea ice cover, but the role sea ice plays in modifying global circulation of the atmosphere is not yet quantitatively understood. The ice cover suppresses drift currents and wind mixing and reduces heat exchange between the atmotphere and the ocean by suppressing heat loss of the ocean to the atmosphere in winter and by reflecting solar heat in summer. The dynamic and thermodynamic interaction of ocean and atmosphere is critically affected by the absence or presence of sea ice. This interaction affects polar regions and perhaps global atmosphere as well (1).

Oceans around some of the countries in the northern hemisphere are covered all or part of the year by sea ice. Most of the cargo between these countries is moved by sea and so sea ice affects trade. Marine operations in the ice frozen oceans require up-to date information on the extent, position, thickness, and break up characteristics of sea ice.

The present interest in the use of radar system to monitor sea ice is primarily developed because of a real need to extend the shipping season into the winter months. The feasibility of achieving this depends to a large extent on making improvements in the ice information gathering techniques. It is quite important that quick, accurate, and comprehensive information on the position, extent, and relative thickness of ice cover with the location of open water areas be made available to shippers on a timely and regular basis so that shipping routes for navigational purposes may be optimized. Moreover, sea ice parameters are also needed to forecast drift and growth patterns of ice cover and its effect on the environment, through the use of meteorological and climatological models. This requires repeated, and in some cases daily, reconnaissance of ice cover. In view of the tremendous aerial extent of the ice cover, the repeated and timely surveillance can be only provided by means of remote sensing techniques. It is in this regard that the allweather, day/night ope-

rational capability and broad aerial coverage provided by a Side-Looking Airborne Radar is seen to be particularly useful and attractive.

Sea ice was first mapped in the early 1960's by SLAR when the Cold Regions Research and Engineering Laboratory (CRREL) conducted experiments over the Arctic pack ice utilizing the AN/APQ-56 radar system. It was shown then by Anderson (2) that sea ice types can indeed be identified on the SLAR imagery. This led the U.S. Coast Guard, during September 1969, in conjunction with the MANHATTAN tanker test, to conduct ice mapping experiments in the Northwest Passage using a Philcoford AN/DPD-2 SLAR operating in the Ku-band (wavelength, $\lambda \approx 1.82$ cm). It was shown by Johnson and Farmer (3) that overall ice conditions, individual ice floes, floe size and number, and water openings can be detected. In addition, it was demonstrated that SLAR imagery can be used to detect ice age, ice drift, surface topography, fractures, relative ice thickness, and pressure characteristics, through careful image interpretation (4). Since then a number of studies have been conducted such as by Raytheon Company (5 and 6) and Photographic Interpretation Corporation (7) to show that SLAR indeed is a useful tool to map changing nature of sea ice. Glushkov (8) and Loshchilov (9) demonstrated the use of SLAR imagery obtained from the satellite 'TOROS' in determining the ice conditions and ice drift. An analysis of multifrequency SLAR imagery of sea ice was conducted by Ketchum and Tooma (10).

The ability of the Side-Looking Airborne Radar (SLAR) to map sea ice has been demonstrated to some extent. The Soviets are already using SLAR for operational ice surveillance. In an effort to understand and define the nature of radar return from sea ice and operational parameters of radar, radar scatterometer data were analyzed in great detail by Rouse (11) and Parashar and others (12). Parashar also correlated scatterometer data with SLAR imagery and developed an analytical model of radar scattering from sea ice. The theoretical results were shown to be in general agreement with the experimental results (14).

The encouraging results obtained in mapping sea ice by radar prompted the use of SLAR in mapping lake ice. Unlike sea ice, which contains salt, lake ice is a fresh water structure. In a report prepared by Photographic Interpretation Corporation (7) for U.S. Coast Guard it was shown possible to detect, delineate, and describe several lake ice types through a detailed, systematic study of the available radar imagery. On a series of X-band SLAR images obtained by NASA Lewis Research Center (15), it was possible to identify lake ice types such as brash, pancake, and related forms because of their brightest return. Radar lake ice data were also reported by Larrowe and others (16).

A review of the above would indicate that the ability and the potential of SLAR in mapping ice has been proven to some extent. What is lacking is the knowledge about the optimum operating parameters of radar such as frequency, polarization, angles, and resolution cell size which would help in the design of an ice mapping radar system of general utility.

2 Formation of Sea Ice

The formation of sea ice is a complex process and is primarily influenced by the brine content of the surface water, the vertical distribution of salinity, surface temperature, and the depth of water. Other factors which influence the formation of sea ice are wind, currents, sea state conditions and the rate of cooling. Sea ice starts to form earlier on the surface of shallow than on deep water, so under similar conditions the ice begins to form near the coast first (17). The amount of salinity present determines the temperature of maximum density. In water with a salinity of less than 24,7 ‰ the temperature of maximum density lies above the freezing temperature. The freezing temperature of water decreases less rapidly than the temperature of maximum density with increasing salinity. The temperature of maximum density in pure water is +3,98° C. Both the temperatures, of freezing and maximum density, are the same at —1,33° C in water of a salinity of about 24,7 ‰. Thus, cooling of a layer of water with a salinity of less than 24,7 ‰ causes an increase in the density of water at the surface resulting in free convection. With continued cooling, this convection continues until the complete convective column reaches the temperature of maximum density for that particular salinity (18). The convection stops at this time. Further surface cooling without mechanical mixing, creates a stratification in a very thin stable surface layer of low density where ice formation rapidly begins when the temperature of freezing point is reached.

The amount of brine present in the water affects the initial freezing of water. But once the freezing starts, the initial ice cover proceeds to from independent of the salinity of the water. The process of freezing can be delayed if the winds produce ocean currents which carry the warmer water to the surface. The amount of turbulent mixing of the water in the freezing layer is the determining and controlling factor in the formation of ice cover.

The first sign of formation of sea ice varies according to different conditions to which the water is subjected. Under calm conditions, the initial ice growth starts after water has been supercooled slightly. The first crystals to form are minute spheres of pure ice and as these grow they rapidly change their shape to circular disks. At some critical diameter, which is about 2 to 3 mm in fresh water and decreases with increasing salinity, the disk form changes to dendritic hexagonal star. These stars grow rapidly across the surface of calm water until they overlap and freeze together to form a more or less uniform sheet of ice, known as young ice. Surface needles are more common in fresh water ice than in sea ice (18).

On the other hand when waves or strong currents disturb the sea surface, the first sign of the sea surface freezing is an oily, opaque, appearance of water. This is known as grease ice and upon further freezing develops into nilas or ice rinds. Some turbulence during initial ice formation introduces more nuclie into the area of active freezing so that the initial crystals are mixed throughout a depth of up to several meters. Snow falling on the water surface, during calm conditions, just prior to and during initial freezing conditions also helps in the formation of similar crystal aggregates. Ice, known as pancake ice and slush is formed because of packing of ice crystals due to wave motion and the general motion of the aggregates against one and other. The thickness of initial ice cover when a slush layer congeals is usually several centimeters. Sheet ice will develop beneath the pancakes and slush ice once a composite ice sheet is formed between the pancakes. The sheet of ice is normally less than 30 cm thick. It is difficult sometimes to distinquish slush ice from infiltrated snow ice, which is formed because of abundant snow fall. The thickness of ice may grow to 10 or 15 cm within 48 hours after which the growth is slower. First year ice which is of one winter's growth seldom becomes

more than 2 meters thick. Sea ice may attain greater thickness through ridges, hummocks, and rafting under the influence of wind, currents, waves and pressure. During the growth of sea ice, the impurities in the form of brine are partially rejected to the underneath water. That is why, the salinity of sea ice is always less than the salinity of the original sea water from which it was formed. In the spring and summer, snow cover and sea ice start melting. This continuing thawing produces passages and holes into which surface water drains.

There are several systems of classification of ice forms. The most widely used system is WMO terminology (19).

2.1 Characteristics of Sea Ice

Sea ice differs from fresh water ice in that it has impurities contained in it sice matrix. The impurities present are in the nature of liquid brine inclusions and are commonly called brine pockets of sea ice (20). The amount of salt or the percent brine volume initially trapped in the sea ice is dependent on the salinity of the original sea water and the rate of cooling. If the water is cooled rapidly, more brine is trapped. The amount of brine present can be found from the phase diagram given by Assur (21). A decrease in the temperature results in the decrease of the relative volume of the brine. The standard salinity profiles (variation of salinity with depth) for different thicknesses of first year ice which have characteristic 'C' shape are given by Weeks and Assur (18). The temperature also varies with depth.

The physical properties of sea ice change significantly with time and age. The physical properties such as salinity and temperature determine the electrical properties.

The electrical properties of fresh water ice or pure ice have been investigated by many workers (22). The most interesting properties of pure ice are its high static dielectric constant (about 100) and its long relaxation time (about 10^{-4} seconds). For frequencies much greater than 1 MHz, the dielectric constant drops (22) to about 3. Because of the presence of the impurities such as brine pockets, the electrical properties of sea ice are significantly different than those of pure ice. The complex dielectric constant of sea ice is dependent on both temperature and brine volume. The brine volume in turn depends on salinity and temperature. Salinity and temperature change with depth and thickness, so the electrical properties of sea ice are a function of thickness of sea ice and vary with its depth.

The dielectric constant of brine varies from 80 at 10^8 Hz to approximately 34 at 2.3×10^{10} Hz (23). Over this entire frequency range, the dielectric constant of the inclusions (brine) is thus several times larger than the dielectric contant of the continuum (ice $\approx$ 3,5). Hence, the dielectric constant of the mixture, that is sea ice, can vary significantly with brine volume dependening on temperature. The same thing holds for the dielectric loss (imaginary part of coemplex dielectric) which can be as high as 20 or more at 4×10^8 Hz at a salinity of 10 ‰ (23).

So, what is clear from above is that the complex dielectric constant of sea ice varies with salinity and temperature and has its own vertical profile.

3 Radar Scattering

Radar is an active system, which transmits its own electromagnetic energy and measures the energy reflected or scattered back from the target. Being an active system it can operate at any time during day or night. Moreover, its operation is independent of almost all weather conditions. This day/night, all weather, operational capability is particularly useful in the regions such as the northern hemisphere, where weather and light conditions are uncertain most of the time.

The density, brightness, or graytone on a radar image is directly proportional to the received power, which inturn depends on the radar backscatter coefficient. This relationship can be expressed in terms of radar equation (24):

$$D \propto \log \bar{P}_r$$

$$\bar{P}_r = \frac{P_t G^2 \lambda^2 \sigma^\circ \Delta A}{(4\pi)^3 R^4}$$

where,

D = Density on the radar image
$\bar{P}_r$ = Average received power
P_t = Transmitted power
G = Antenna gain in the direction of ΔA
λ = Incident wavelength
R = Range to the resolution cell of area ΔA
σ° = Radar backscattering coefficient or backscattering crosssection per unit area of the target

Each small area on the ground equal to a resolution cell size Δ A produces one point on the image. In a real-aperture SLAR, the resolution cell size in the along-track direction is determined by the beamwidth of the antenna and the range to the resolution cell. It increases with increasing range. The beamwidth of an antenna is directly proportional to the wave length and inversely to the length of the antenna. In other words a fine resolution in the azimuth or along-track direction can be achieved by either decreasing the range, decreasing the wavelength, or increasing the antenna length. The acrosstrack resolution or range resolution depends on transmitted pulse length. The smaller the pulse length, the smaller resolution is achieved. In a synthetic-aperture radar a better resolution in the azimuth is achieved through synthetically obtained large antenna. This is obtained by storing both the amplitude and phase of the return signal and adding the signals coherently (25). As a result, for a focussed radar, a small resolution in the azimuth is achieved which is independent of the range and wavelength and is equal to half the physical length of the antenna (24). A synthetic-aperture radar is obviously more complicated and expensive than a real-aperture radar.

Except for the quantity σ°, all the othed parameters in the radar equation are either system or flight parameters. So, essentially, it is the variations in σ°, which are depicted as variations in density or brightness on an image. The linking parameter between the brightness on a radar image and the properties of the target is the quantity σ°. Target here is implied both discrete and continuous like terrain. Thus, it is because different targets have different values of σ° that they appear different on a radar image. In general σ° depends on wavelength, angle of incidence, and the polarizations of the transmitted and received wave. The value of σ° also depends on such target parameters as surface roughness on the wavelength scale and subsurface structure, complex electric permittivity, and physical and quantum resonance.

When electromagnetic energy or waves hit the earth's surface, the waves may either be transmitted, absorbed, specularly reflected or scattered.

Waves are said to be specularly reflected, when they follow Snell's law in which case the angle of incidence is equal to angle of reflection. Scattered waves have components in all the directions from 0 to 180 degrees. The amount of energy specularly reflected or scattered depends on the surface roughness of the target, the wavelength, and the angle of the incident wave. A measure of the surface roughness is the size of surface height irregularity or variation in comparision with the wavelength of the incident radio wave. A change in the surface configuration from smooth to rough would result in the decrease of the specularly reflected wave relative to the non-specular or scattered wave. The energy or signals returned along the same path as the incident energy is called the backscattered. The specular reflection at microwave lengths, at which radars operate, is usually very small as compared to the scatter waves in the case of backscatter. Thus the radar measures the returned power, which is dependent on radar backscatter coefficient.

A perfectly smooth surface gives return only in the specular direction. A surface is generally said to be smooth if $\Delta h < \frac{\lambda}{8\cos\theta,}$ where Δh is surface height variation, λ is the wavelength of the incident wave, and θ is the angle of incidence. With a very rough surface, the scatter is almost uniform in all the directions including the source. For a slightly rough surface most of the incidence energy is scattered near the specular direction. Thus, a surface which is smooth at one frequency may not be smooth at higher frequency. The same surface will appear rougher as the wavelength of the incident energy is decreased. The degree of surface roughness determines the slope of σ° vs θ curve at a particular frequency corresponding to transmitted and received polarizations. That is, the smoother the surface, the faster is the drop in the value of σ° as the incident angle θ changes from near vertical to near grazing. For a rough surface σ° vs θ curve is relatively flat. (See Table I).

In addition to surface roughness, the electrical properties of the medium also play an important part in determining the value of σ°. The complex permittivity (the real part is the dielectric constant and the imaginary part can be expressed as a loss tanget) does not only determine the amount of energy which is scattered or reflected back but also determines the degree of penetration of incident electromagnetic energy. The value of loss tangent and the wavelength determines the attenuation in the medium and thus the skin depth or depth of penetration. The higher is the value of the loss tangent and smaller is the wavelength, greater is the attenuation and hence a smaller skin depth. Thus the choice of frequency determines the depth of penetrations and thereby influences the contributions made by the subsurface structure to the radar return.

In the end it should be pointed out that almost all the SLARs in operation today are uncalibrated systems. Thus, the gray tone, brightness or density on a radar image is relative and not an absolute quantity. For comparing two radar images obtained by utilizing two different systems or the same system, a common reference point for calibration purposes should be established.

3.1 Radar Scattering from Sea Ice

Radar backscatter from floating ice is a combination of scattering from ice-air and ice-sea water interfaces and from irregularities within the ice mass. The relative contribution to backscatter from the two boundaries and the irregularities depends on the frequency, polarizations, angle of incident wave and the electrical and physical properties of sea ice like complex permittivity, surface roughness, temperature, salinity, and thickness. In addition, the absence or presence of some type of snow cover may have some relative effect on the radar return.

By selecting a value of 3.15 for dielectric constant and 10×10^{-14} for loss tangent (pure ice), the skin depth for ice can vary linearly with frequency from about 100 cm at 1 GHz and 10 cm at 10 GHz to 1 cm at 20 GHz. The depth of penetration decreases as the salinity increases because of increase in the value of loss tangent.

An analytical model of radar scattering from sea ice was developed by Parashar (13) by taking into account the surface roughness, the amount of brine entrapped, and temperature. Sea ice was considered as an inhomogeneous medium in which the inhomogeneity in the nature of brine entrapped varies continously in the vertical direction. In addition, it was

considered to have a small random variation in the horizontal direction. Maxwell's equations were solved using the small pertubation method together with Fourier transform techniques. The computed results interms of σ^{o} vs θ for different ice types were shown to be in general agreement with the experimental results. The final σ^{o} equation composed of two terms; surface roughness and inhomogeneity. The major contribution to the radar backscatter at 13.3 GHz frequency was from surface roughness term. This was because of small penetration. The contribution from the inhomogeneity term increases, though relative surface roughness still very small, as the salinity decreases because of a decrease in the value of loss tangent and thereby a greater penetration. The inhomogeneity term drops down relatively faster than the roughness term as the angle of incidence increases (from the vertical zero degree). Thus, essentially, the radar return, from the model, is from the surface roughness, of course, the calculations were made at only one temperature, by assuming the values of inhomogeneity and the surface roughness. The theoretical model need to be tested further for its validity by conducting controlled experiments with the collection of relevant ground truth.

4 "Sea Ice -75" Experiment

During March, 1975, a remote sensing experiment was conducted jointly by Sweden and Finland with the participation of Netherlands in the Bay of Bothnia (Sea of Bothnia) (26). The main objective of the experiment was to evaluate the capabilities and limitations of modern remote sensing techniques for mapping sea ice. Specifically, it was proposed to evaluate from the remote sensing recordings, the primary parameters of sea ice such as presence or absence of ice, ice concentration, ice roughness, ice thickness, state of ice surface, and type of ice. In addition, it was decided to study the effect of such environmental parameters as temperature, cloudiness, wind speed, sea state, and time of the day, on the remote sensing recordings. It was also decided to evaluate the effect of snow cover and gather information about the drift speed and direction. The influence of altitude in the ability to identify different ice types was also proposed to be studied. The purpose of the experiment was and is to gather sufficient information which would help in the design of an operational remote sensing system for ice surveillance.

4.1 Remote Sensors Employed

To help achieve some of the objectives of the experiment a variety and a number of remote sensors were used. These included real aperture SLAR (Side-Looking Airborne Radar), FLAR (Forward-Looking Airborne Radar), and ODAR (Omni-Directional Airborne Radar), all working at 3 cm wavelength. Ship based radars operating at 3 and 10 cm wavelength, radar altimeter at 6 cm wavelength, and microwave radiometer, operating at 6 cm wavelength were also employed to gather the data. Correlating data from SR (Scaning Radiometer) and VHRR (Very High Resolution Radiometer) aboard NOAA-4 satellite along with MSS (Multi-Spectral Scanner) data from Landsat-2 were obtained. High altitude camera, multispectral camera, and IR scanner belonging to Swedish government were also employed. Aerial photography was primarily obtained to act as a ground truth with other ground truth information such as temperature and salinity of ice.

Only the results obtained from the analysis of SLAR data are presented in this report.

4.2 Design of the Experiment

To obtain experience of the capability and possible limitations of various remote sensing techniques, the field experiment was conducted in the Bay of Bothnia (Sea of Bothnia) during the period of 10 to 20 March 1975. The experiment comprised of measurements on two scales:

— specially chosen relatively small ground truth areas
— large area mapped by remote sensors.

The ground truth information was gathered at three different scales. The area for identification purposes was divided into three sections, 1×1 km area, 5×5 km area, and 15×15 km area. Most detailed ground truth was collected for the 1×1 km area. Larger 15×15 km area was mapped by various remote sensors. The smaller areas were contained whithin the larger areas. All the areas were marked by flags, tarpaulins and radar reflectors. The Swedish ice breaker 'TOR' was situated in the middle of the experimental area as an operational base and a reference point. The details of the experiment and the data collected from it are given in reports (26) and (27).

4.3 Sea Ice Parameters of Interest

The main parameters of interest for the navigational, climatological and meteorological purposes are the relative ice thickness, ice surface roughness, ice drift, and general ice conditions. The utility of any remote sensor for providing this information should be judged on its ability to map position, extent, thickness, and roughness of ice. It should be possible to locate open water areas and distinquish ridges. Since pressure ridges are difficult to navigate through, it is important to know their position, spatial extent, height if possible, and direction. It would certainly be helpful to know the location and direction of fractures and cracks. In addition, information about the temperature of the ice surface and the surrounding water would be helpful. The knowledge of the general direction and the rate of the ice drift would be extremely useful in predicting the opening and closing of leads. Information about the presence or absence of snow cover would be advantageous. The effect of snow cover in maskin sea ice signature need to be established.

5 Ground Truth Information

Water in the Sea of Bothnia is of relatively low salinity as compared to the water in the Arctic ocean. The salinity is even lower in the Bay of Bothnia. As a result the sea ice found in the Bay of Bothnia contains very small quantities of brine. As a matter of fact the surface salinity of ice measured during the "Sea Ice -75" experiment was of the order of 0.5 ‰ and smaller. Whereas in the Arctic even multi-year ice, which has gone through at least a summer's melt and is relatively salt free at the surface, is expected to have a surface salinity of at least 1 ‰. First year ice, ice of one winter's growth, can have surface salinity of as much as 15 ‰ or more. Because of the very low salinity, the ice in the Bothnia is expected to start forming relatively earlier in fall and start melting relatively later in spring. Only first year, that is of one winter's growth is found in the Bothnia. In the cold winter this ice may be as much as 1 m thick. Of course, it may attain greater thickness through rafting and pressure ridging.

Thus, as is evident from above, ice found in the Bay and Sea of Bothnia is quite different from that found in the Arctic and this fact should be borne in mind when the results presented here are compared with past measurements from the Arctic. Sea ice in the Bothnia consists of relatively more pure ice and should be comparable to ice found in the Great Lakes and other lakes.

Typical thickness of level ice expected to be found during a normal winter is 50—70 cm in the Bay of Bothnia and 20—40 cm in the Sea of Bothnia (28). In the Bay of Bothnia pressure ridges as high as 2 m often appear and ridges 5—6 m high have been observed. The winter during 1975 was extremely mild with mean temperatures 4—5° C above normal in the Bay and Sea of Bothnia. The mean temperature varied from —0,6° C in the south of the Bay to —50° C in the north. As a result the maximal ice extension was much less than normal and the thickness of level ice was 20—40 cm. Normal salinity values in the water in the Bay are about 3—3,5 ‰ and in the Sea of Bothnia about 5—5,5 ‰ (28).

The ice charts in detail showing ice concentration and level ice thickness during the period of the experiment are given by Udin and Omstedt (28). A detailed analysis of the ground truth information collected during the experiment is provided by Udin (29).

Small-scale thickness measurements were made in a 1×1 km area around the ice-breaker 'TOR'. The ice thickness was measured every 200 m but along one line in the area, holes were drilled to measure thickness every 10 m. The measurements do show a considerable variation in thickness over a rather small area. The thickness of level ice, without rafting or pressure ridging, was 25—30 cm but the mean value over the area was 43,5 cm. In addition to these, spot measurements of ice thickness were also made. Small pressure ridges had a thickness of 1 meter. The wind speed during the period, March 10—15 was less than 10 m/s, increasing to 19 m/s on March 16. It decreased during the 17th and increased again on March 18 to 15 m/s.

The mean salinity in level ice was found to be 0,435 ‰ in the layer of 2—7 cm, 0,292 ‰ in the layer of 8—13 cm depth, 0,440 ‰ in the layer of 14—19 cm depth, and 0,251 ‰ in the layer of 20—25 cm depth from the top surface. There was no snow fall during the experiment.

The National Land Survey of Sweden also participated in the experiment by providing medium to low level photography of the ground truth areas with a purpose of correlating it later with the various remote sensor recordings. For such a purpose a Wild RC-8 camera with an UAg 152 was used. It produced 23×23 cm photographs. The Wild camera was used to provide aerial photographs of the 15×15 km area on March 14

and 17. In addition, a Hasselblad camera package producing 6×6 cm photograph was used to provide aerial photographs of the 5×5 km area on March 13 and 18. This report is mainly concerned with the SLAR data collected during three of those days. To facilitate identification of the ice types and general ice conditions, mosaics were made from the individual aerial photographs to depict the entire experimental area.

6 SLAR Data

Radar imagery during the experiment was obtained by utilizing an EMI X-band real-aperture SLAR (Side-Looking Airborne Radar) operating at a frequency of 9,6 GHz with horizontal-transmit and horizontal-receive polarizations. The radar was carried aboard a Beechcraft Queen Air 80 laboratory aircraft belonging to the National Aerospace Laboratoys (NRL) in the Netherlands. The maximum altitute obtainable is about 6000 m with a speed of 240 km/hr. This SLAR was developed originally as a navigation radar for the British military aircraft TSR-2. Data are reproduced on film. The operational details of SLAR are given by Morra and de Loor (30).

Some of the operational parameters of radar are given below:

Power output (nominal)	80 kW peak, or 25 kW in low level rote
Pulse duration, τ (nominal)	0,2 μsec
PRF	1260 or 2520 Hz, depending on range
Antenna system	Slot radiators in 7'6" long antenna fitted with a horn; double. Available: single antenna ditto 15' long
Antenna pattern	Cosec² (imperfect)
Beamwidth (elevation)	36° at 6dB, 23° at 3dB points
Beamwidth (azimuth)	56' at 3dB points
Display	Intensity modulated scan on a CRT photographed on 5" wide sensitized paper and rapidly processed. Film system (negative) available
Display map scale	At low level 50 k:1 and 100 k:1 corresponding to 3,15 and 6,3 km, both sides. At medium level 200 k:1 and 500 k:1 are used corresponding to 25 and 65 km respectively (one side only).

Radar was operated in two modes. In the first mode 6,3 km swath width was mapped on both sides of the aircraft with a gap directly underneath the aircraft. In the second mode, a 25 km swath width was mapped on only one side of the aircraft. The geometry of radar mapping is shown below in Figure 1.

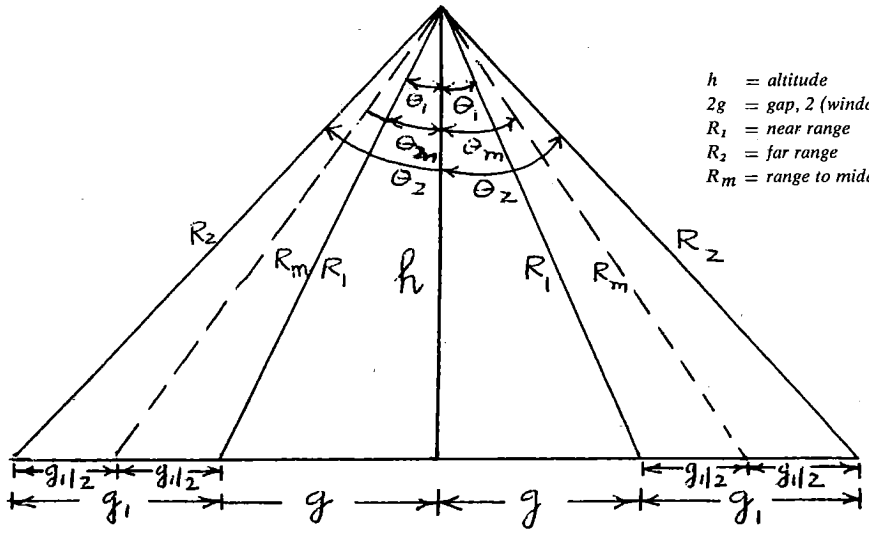

Figure 1. *Geometry of radar mapping.*

h = altitude
2g = gap, 2 (window shift)
R_1 = near range
R_2 = far range
R_m = range to middle of image
g_1 = swath mapped
θ_1 = near range incident angle
θ_2 = far range incident angle
θ_m = mid range incident angle
$g_{1/2}$ = mid swath

Across-track resolution cell $\gamma_{ac} = \frac{C\tau}{2 \sin \theta}$

For, $\tau = 0{,}2$ μsec, *and* $C = 3 \times 10^8$ *m/sec,*
$\gamma_{ac} = \frac{30}{\sin \theta}$

Along-track resolution cell, $\gamma_{al} = R \varnothing$
For beamwidth $\varnothing = 56'$ $\gamma_{al} = 15\, R_{km}$ *m*

The data were presented in the slant range mode. Five different altitudes were used. For altitudes including 1300 ft and less, data on the original images were mapped at a scale of 1:100 000, with a swath width of 6,3 km on both sides of the aircraft. For altitude of 20 000 ft, images were mapped at a scale of 1:200 000, with a swath width of 25 km on one side of the aircraft. Different parameters, including ranges and angles corresponding to different altitudes are presented in Table I.

Table I. *Different parameters, including ranges and angles, corresponding to different altitudes.*

h	h	g	θ_1	R_1	g_1	$g+g_1$	θ_2	R_2	$\gamma_{al(n)}$	$\gamma_{ac(n)}$	$\gamma_{al(f)}$	$\gamma_{ac(f)}$	g_m	θ_m	R_m	$\gamma_{al(m)}$	$\gamma_{ac(m)}$
ft	m	km	deg	km	km	km	deg	km	m	m	m	m	km	deg	km	m	m
500	152.4	1.852	85.29	1.853	6.3	8.152	88.92	8.153	27.79	30.1	122.29	30.0	4.0	87.81	4.0	60.0	30.0
900	274.3	1.852	81.57	1.87	6.3	8.152	88.07	8.155	28.05	30.3	122.32	30.0	4.0	86.08	4.0	60.0	30.0
1000	304.8	1.852	80.65	1.87	6.3	8.152	87.85	8.157	28.05	30.3	122.35	30.0	4.0	85.64	4.0	60.0	30.0
1300	396.2	1.852	77.92	1.89	6.3	8.152	87.21	8.23	28.35	30.92	123.45	30.3	4.0	84.34	4.04	60.6	30.3
20,000	6.096	0.482	46.75	8.89	25.0	31.48	79.04	32.06	133.35	41.18	480.9	30.3	18.90	72.12	18.93	283.95	31.52

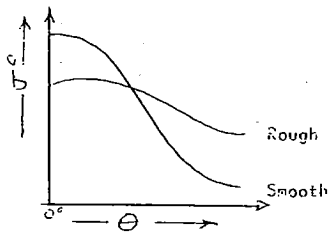

$g_m = g + g_{1/2}$

(n) = near range

(f) = far range

(m) = mid range

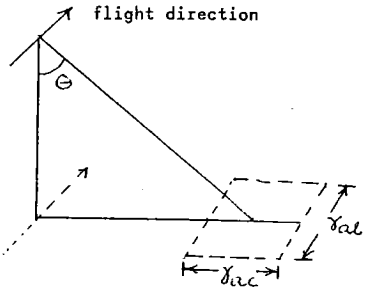

Sea ice was mapped with SLAR during five different days and each day was assigned a flight number. The details corresponding to each flight are shown in Table II. The areas covered during each flight are shown in Figures 2 and 3. Two lines were flown in the west-east direction and two in the northsouth direction. Two intersecting lines were flown over the ice breaker 'TOR'. The lines were not exactly perpendicular or parallel as shown in the diagram and even the spacing between the lines varied. Sometimes diffferent altitudes were used for different lines and the details of the flight heading, altitude and location can be found in (31). It was hoped that the imagery obtained from parallel lines would overlap but only in some instances it does. In flight 952, only one run was made over 'TOR' as given in Table II.

Table II. *SLAR data collected during SEA ICE -75 Experiment.*

FLIGHT NO.	DATE	TIME	SCALE	ALTITUDE	COVERED AREA
950	12-3-1975	14.45 - 16.00 h	1:100.000 Band Width 2 x 6,3 km	300 m	Swedish 15 x 15 km area Preliminary tests
951	13-3-1975	13.00 - 14.30 h	1:100.000 1:200.000	300 m	Swedish 15 x 15 km area 1 run on track 270° S of TOR
952	14-3-1975	11.00 - 13.00 h	1:100.000	400 m	1 run over TOR → Malören → Bjuröklubb → east southeast to Finnish coast → north to Malören → Luleå
953	18-3-1975	11.00 - 12.00 h	1:100.000	150/300 m	Swedish 15 x 15 km area
	"	12.00 - 13.30 h	1:200.000 Band Width 1 x 25 km	6000 m	65.30N, 23.00E → Gasören → east to 64.40N, 23.10E → north to 65.30N, 23.10E covering Finnish and Swedish 15 x 15 km areas → Luleå
954	19-3-1975	13.15 - 15.30 h	1:100.000	150/300 m	Swedish and Finnish 15 x 15 km areas.

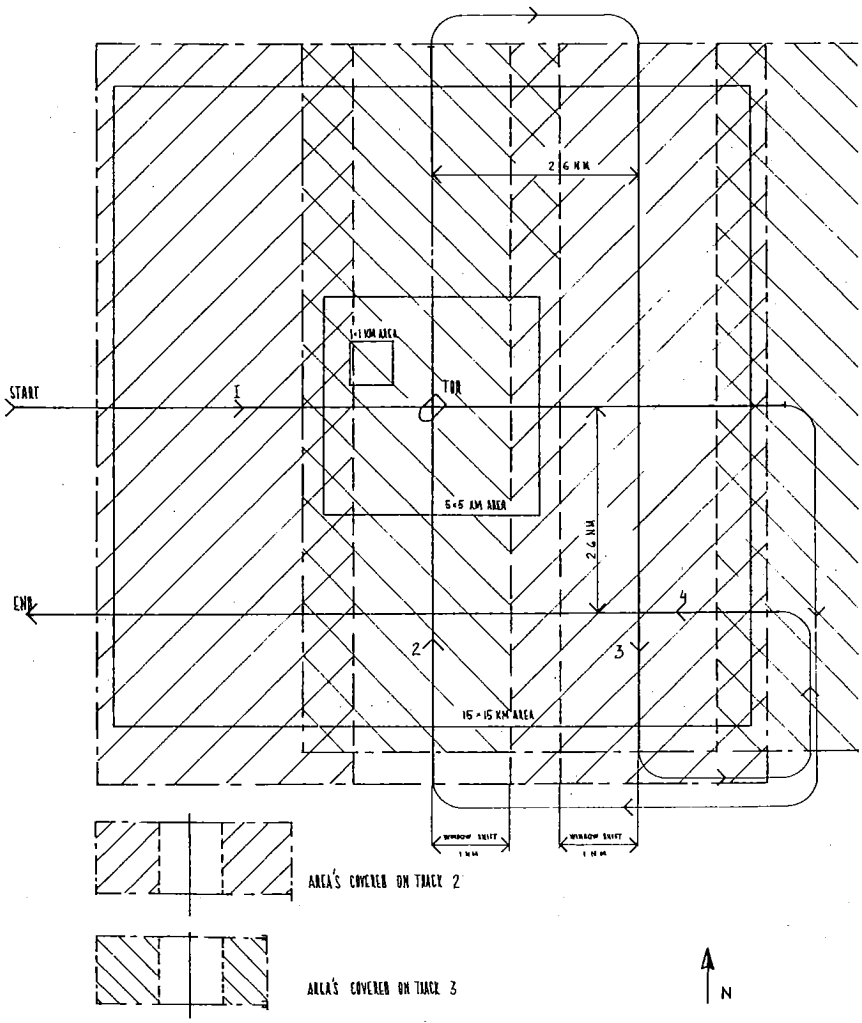

Figure 2. *Flight pattern and area mapped (Flight 950).*

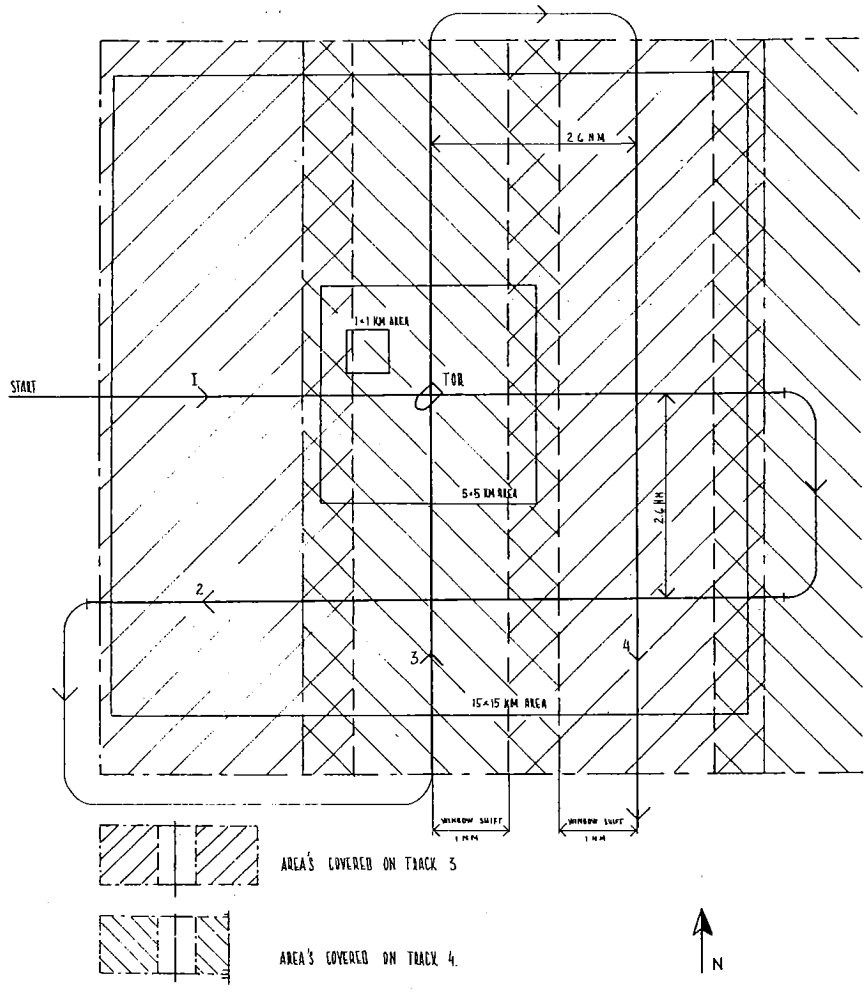

Figure 3. *Flight pattern and area mapped (Flights 951, 953, 954).*

7 Preliminary Analysis of SLAR Data

Positive prints were made from the original negatives and some of these are shown in Figures 4, 5, 6, 7, and 8. A cursory examination of these images would show that the images are of moderate quality. Though, most of the features are mapped consistently from image to image. The data are presented in the slant range mode but the change of the scale from the near range to far range because of change in the acrosstrack or range resolution is not evident. Center line is the near range. It is because, the images are obtained by operating the radar at near grazing angles with a variation of 3 to 8° over the entire image depending on the altitude. As a result there is no significant change in the range resolution cell size from near range to far range as is evident from Table II. There are some changes in the along-track resolution cell size from near-range to far-range and these sometimes are apparent when comparison is made with mosaic. The changes in scale because of non-square resolution cell size in the far-range are evident when a comparision is made between the same area mapped by two perpendicular flight lines.

Even though the radar was operating at less than the maximum range, there is a loss of signal in the far range. This could very well be due to the imperfect cosec^2 antenna pattern. Otherwise there is no detrimental effect of antenna pattern. The gain of the system was kept almost the same throughout most of the experiment, but still there are certain instances of gain variations. Sometimes vertical scan lines and streaks are visible and certain cases of complete image wash out are apparent. There are certain examples of missing data, especially, near the ice-breaker 'TOR'. But these are probable operative controlled faults. These are likely present because of an effort to align the aircraft heading with or over 'TOR'. The first thing which immediately strikes the eye when it looks at the images is the lack of gray tone or density variations. Most of the imagery is either over-saturated or under-saturated. This is a case of dynamic range, gain control, and sensitivity problem.

It should be pointed out that even though SLAR operates at microwave frequencies, the final output is in the visible part of the spectrum, that is, a black and white image. Thus, the SLAR image represents, essentially, a transformation from the lower part of the electromagnetic frequency spectrum to the higher part so that our eye can see. To fully appreciate the role photographic process plays in the final output, it would be helpful to examine this transformation. This would help point out some of the inherent limitations of a photographic film.

A very short pulse of electromagnetic energy at the microwave frequency is transmitted by the radar antenna in the area illuminated by it. The illuminated area is wide in the across-track direction and narrow in the along-track direction. The size of these areas are determined by the size of the antenna. One small strip of the ground is swept by this pulse. The echoes received back by the antenna arrive at different times because of diffferent ranges in the across-track direction. By determining the difference in arrival time between different echoes, the corresponding ranges can be ascertained because of fixed velocity of electromagnetic wave. The ranges separated in time duration by less than the pulse length determines the range or across-track resolution in a simple system. For a real-aperture radar, the along-track resolution is determined by the narrow illuminated region. A successive pulse is sent when the antenna illuminates an adjoining strip because of the movement of the antenna with the aircraft. The whole process is thus, repeated. One illuminated strip appears as vertical line on the film. By moving the film at the same speed as that of the aircraft the whole area can be imaged continuously.

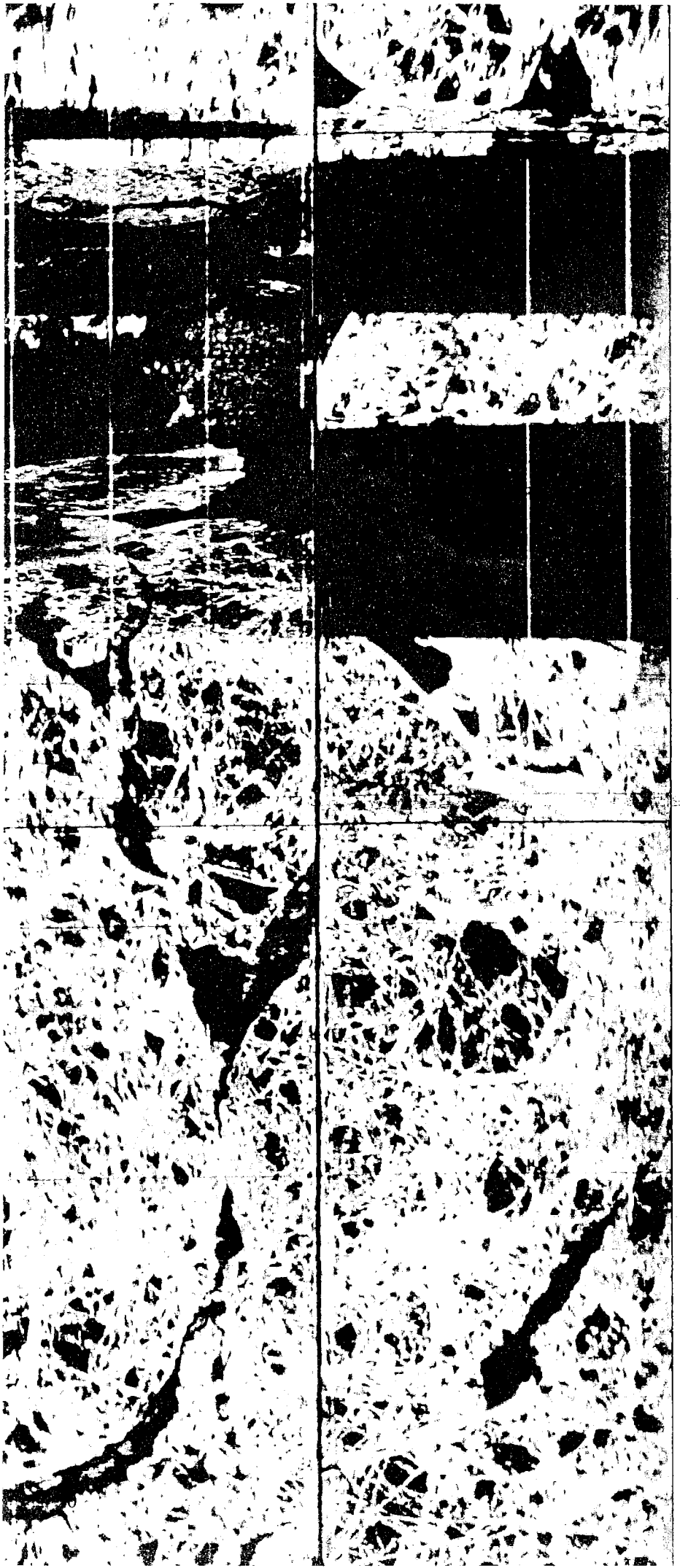

Figure 4. *Radar image showing open water, level ice, and very rough ice (1:100.000, Flight 953).*

Figure 5. *Radar image showing level ice, ridges, open water, and very rough ice (1:100.000, Flight 951).*

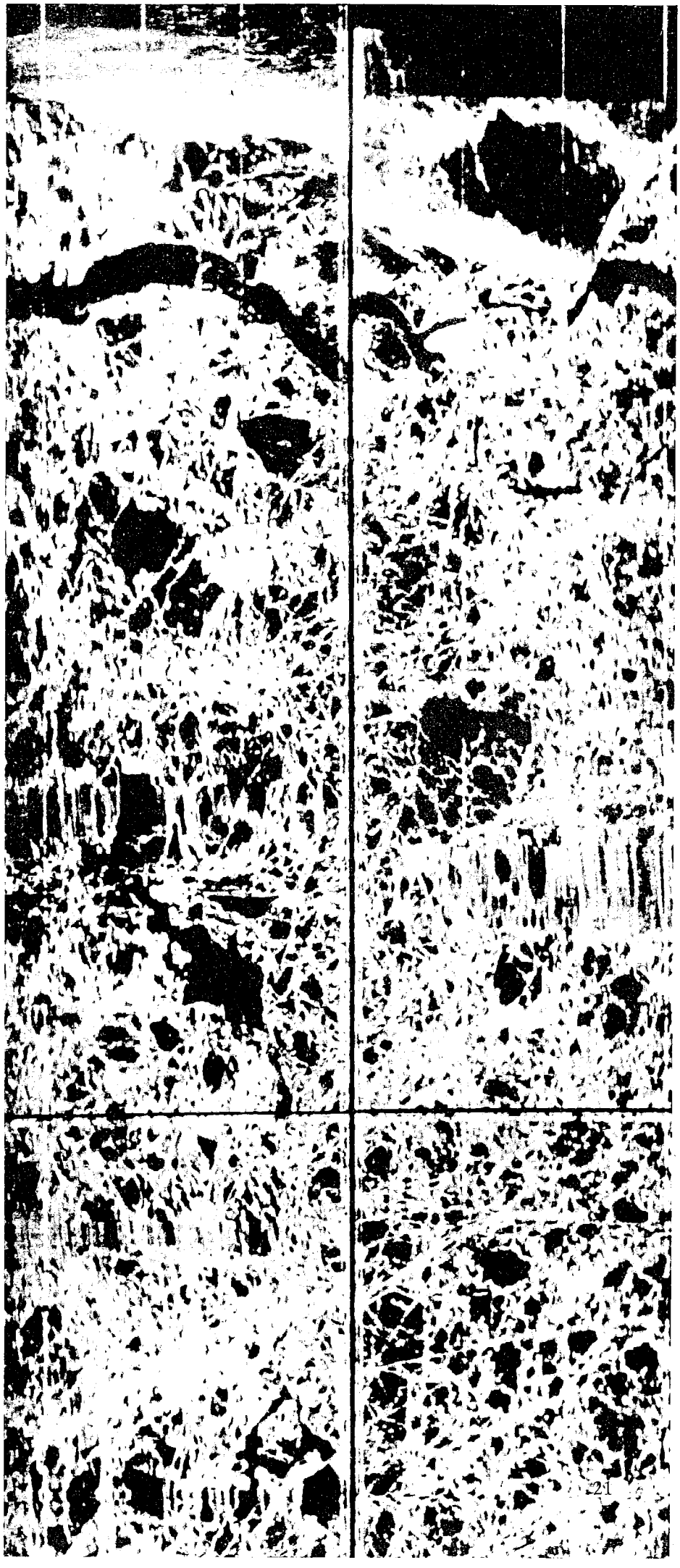

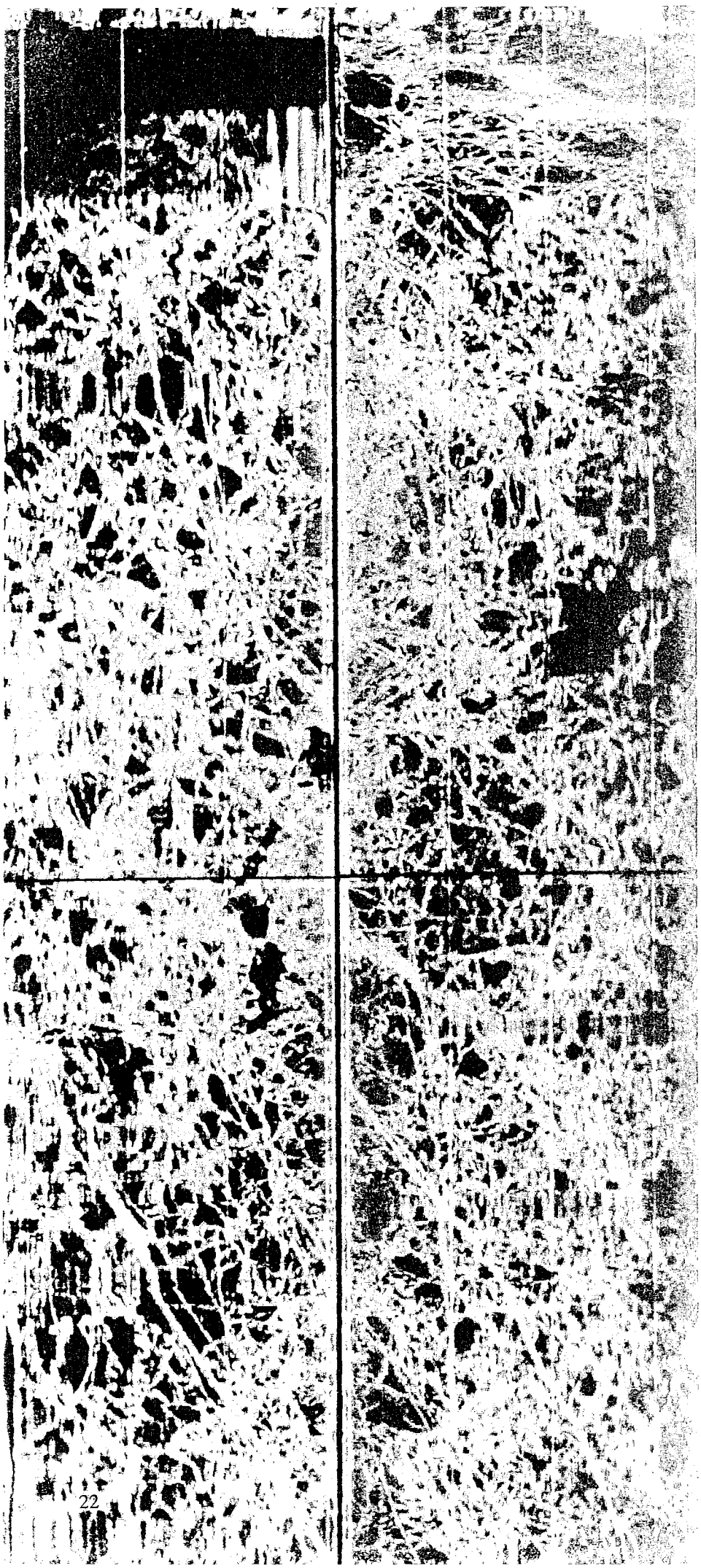

Figure 6. *Radar image showing ship's tracks, level ice, ridges, open water, and very rough ice (1:100.000, Flight 951).*

Figure 7. *Radar image showing level ice, open water, and ridges (1:100.000, Flight 952).*

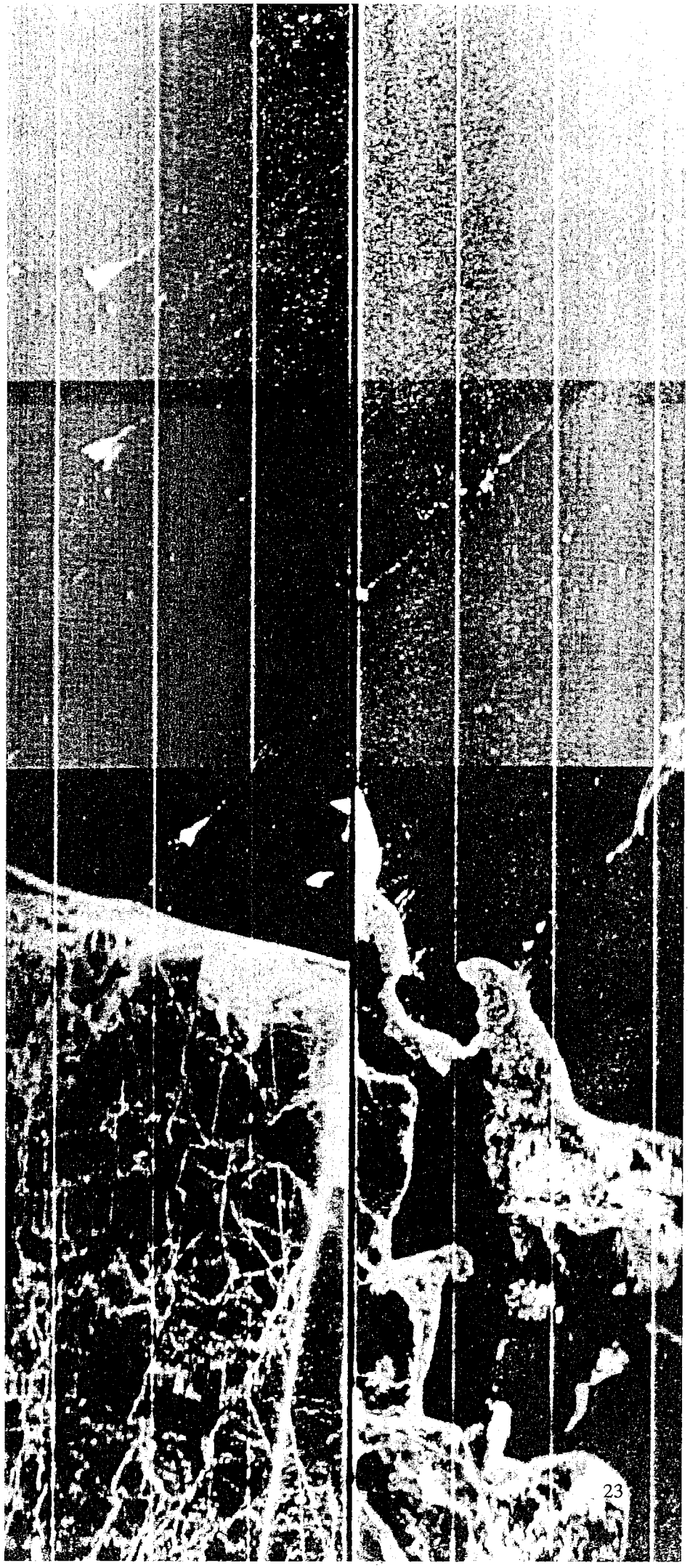

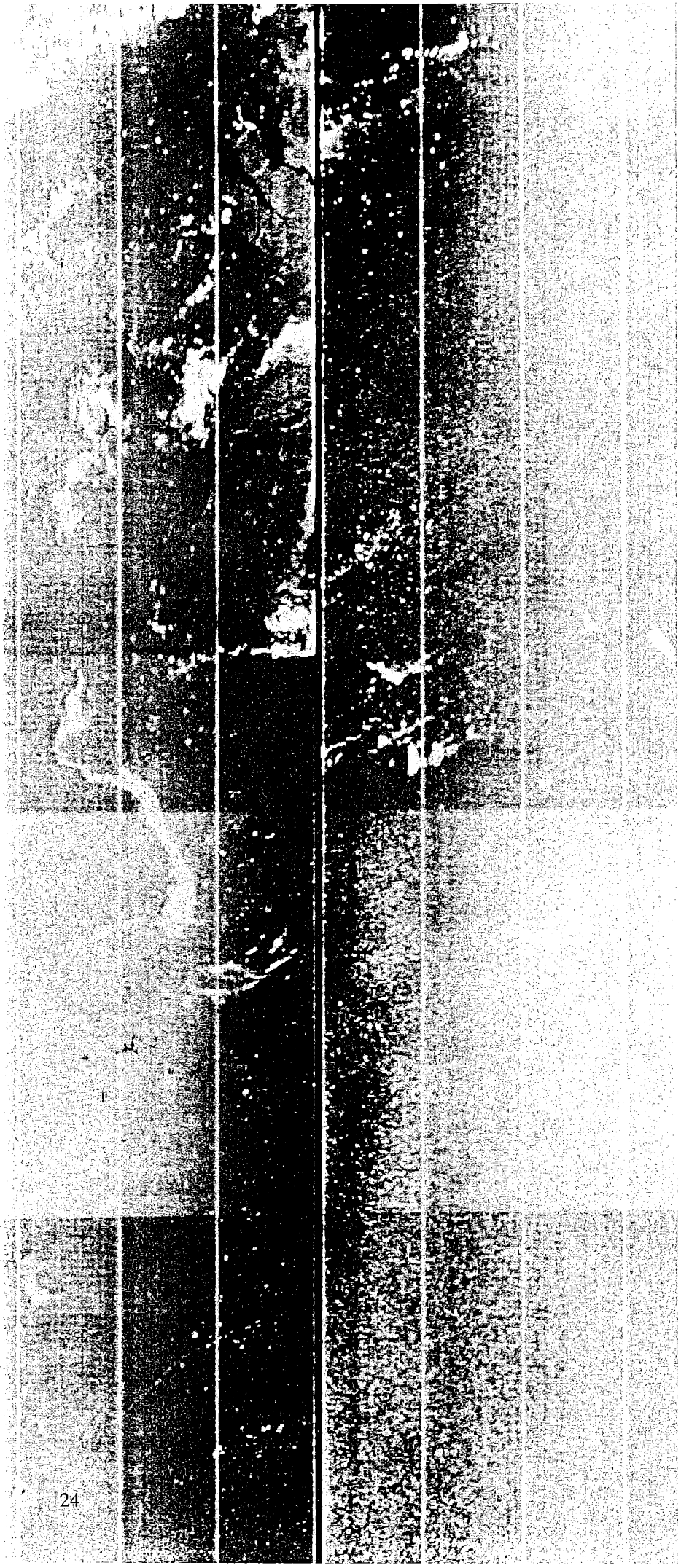

Figure 8. *Radar image showing open water with slush (1:100.000, Flight 952).*

So, what the radar measures is the average received power scattered back by the small area of the size of the resolution cell. This average power appears as an intensity modulated dot on CRT which is used to expose the photographic film. The transformation of information on to a film is determined by the characteristic curve or D and E curve of the photographic film. This curve is shown below (Figure 9) and is a plot of density on the film and log E, where E is the exposure.

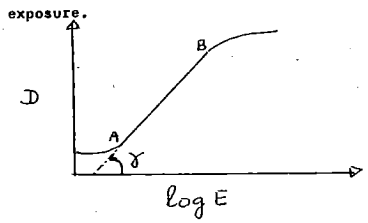

Figure 9. *Characteristic curve of a photographic film (log E).*

$E = IT$
where, I = *Intensity* $\propto \bar{P}r$,
$\bar{P}r$ = *Average received power*
T = *Exposure time*
Thus, $D \propto \log \bar{P}r$

The slope of the linear portion of the curve is known as 'gamma' of the film, and is a measure of the contrast. The length of the linear portion (AB) of the curve is called the dynamic range and determines the maximum and minimum intensity that can be linearly represented. Thus, when the average received power falls above the linear portion, it is a case of oversaturation, and when it falls below, it is a case of undersaturation. A photographic film can have a dynamic range between 20—30 dB. EMI radar was equipped with a rapid processor unit (RPU) to allow the navigator have an immediate view of the surroundings. The imagery was produced on a film with a paper base, which is claimed to have a dynamic range of 20 dB (30). The dynamic range of the return signal from the very rough to very smooth ice can be much higher than this. So, either the return signal was high or low to be properly represented on the "Sea Ice -75" SLAR images. This problem could be partially alleivated by reducing and controlling the gain of the system. By reducing the gain part of the signals returned could have fallen on straight line portion, thus, showing more detail. But by reducing the gain, the signals from the far range would have become relatively smaller, thereby blacking out this region on the image. It is hoped that the problem does not lie with the dynamic range and sensitivity of the radar system itself. There are certain instances in the radar images obtained where small graytone variations are apparent, especially in the near range.

7.1 Detailed analysis of SLAR imagery

To conduct a detailed and systematic analysis of the radar imagery, it was first decided to consider those images for which aerial photographs were available. This was done so that SLAR images could be properly correlated with the aerial photographs to ascertain what SLAR actually sees and maps. Once this was established, the remaining images could be analysed accordingly.

The aerial photograph mosaics which are available along with the corresponding SLAR imageries are shown in Table III.

Table III. *Available photos and mosaics along with corresponding SLAR imageries.*

Date March	Flight No.	Mosaics		High alt. photography	Mosaic scale	SLAR scale
		5x5 km	15x15 km			
12	950			X		1:100 000
13	951	X			1:10K	1:100 000
14	952		X		1:20K	1:100 000
17			X	X	1:20K	1:100 000
18	953	X			1:10K	1:100 000
19	954					1:100 000

5×5 km mosaics were made with the individual photographs obtained by the Hasselblad camera and 15×15 km mosaics those obtained by Wild RC-8 camera.

To begin the analysis, 5×5 km mosaic corresponding to March 18, was selected. The first step was to divide the ice in this mosaic into a number

of categories, which were later termed photographic categories. These categories were formulated by keeping in mind the needs and objectives of the experiment. It was felt that if these categories could be identified on the SLAR imagery, then SLAR imagery could indeed provide useful and sufficient information about ice. It was realized that these categories were rather too fine, too detailed, and too many but it did provide the starting point. Ice in the 5×5 km area was divided into these categories strictly on the basis of ground truth information available and their appearance on the aerial-photo mosaic. Categorization of ice into categories was started with the 1×1 km area for which a detailed ground truth information was available. Ice in the surrounding area was then delineated accordingly. As a result the following eight photographic categories were identified on the mosaic:

Category 1: Open water
Category 2: New ice (thickness less than 5 cm)
Category 3: Level ice (thickness above 5 cm)
Category 4: Rafted ice
Category 5: Light to moderate ridged ice, areal coverage less than 50 %
Category 6: Light to moderate ridged ice, areal coverage more than 50 %
Category 7: Heavy ridged ice, less than 50 %
Category 8: Heavy ridged ice, more than 50 %
(Heavy ridge: at least 1.5 m high above the surface)

In addition, it was considered appropriate to put suffix 'A' to each category to distinguish areas with any snow cover. This was thought desirable so as to determine the effect of presence or absence of snow cover on the SLAR imagery. The details of the categorization of ice into photographic categories is given by Udin (29) in a report on the available ground truth information.

The mosaic of March 18, is shown in Figure 10. The overlay shows the delineation of ice into photographic categories. The radar image for the corresponding area is shown in Figure 11. An immediate glance shows that the details on the SLAR imagery are insufficient to identify so many categories. As a result it was decided to prepare another overlay for the mosaic to show the areas which appear similar on the SLAR image. The

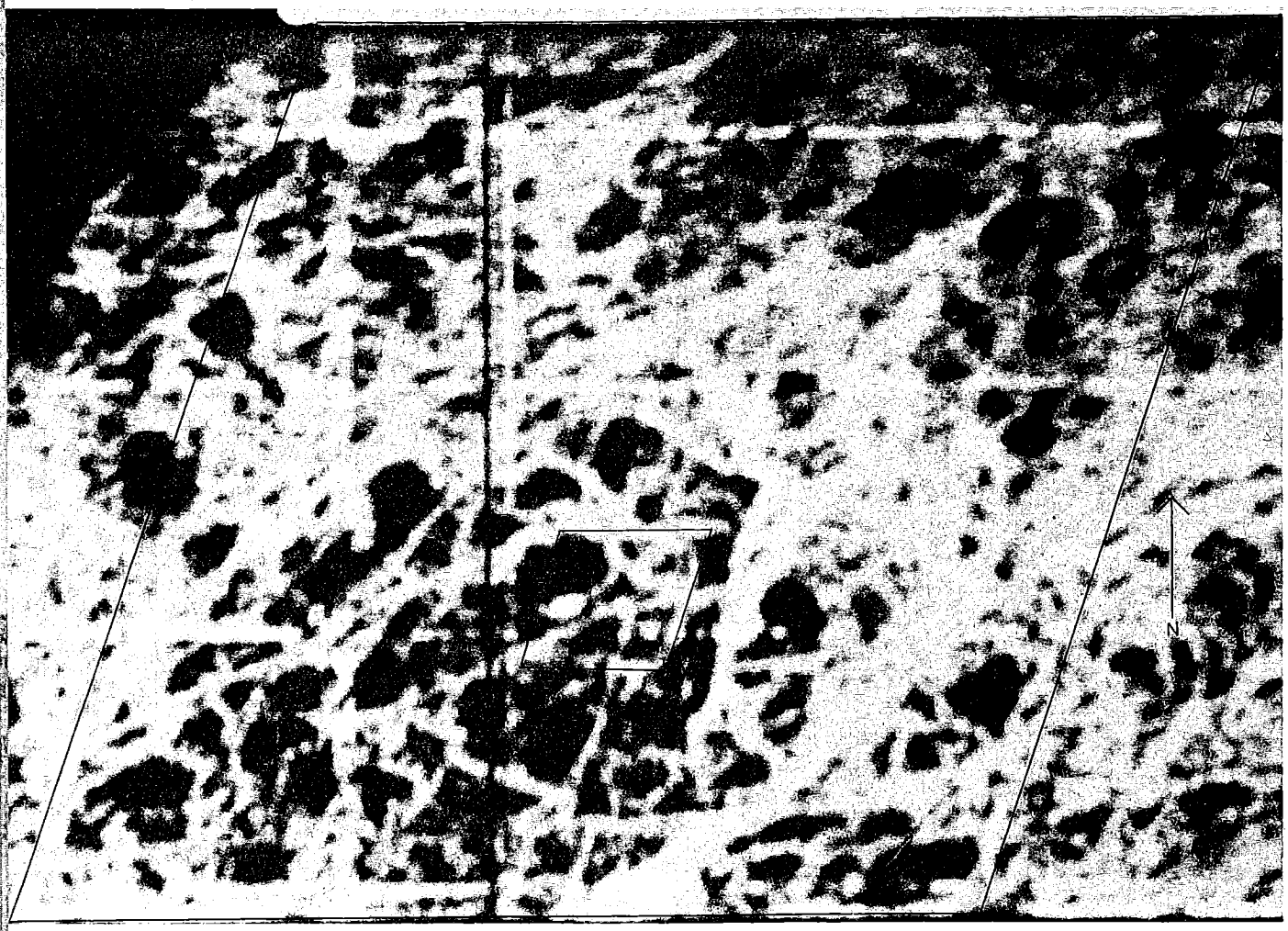

Figure 11. *Radar image corresponding to Figure 10 (Flight 953).*

Figure 10. *Photo-mosaic (5 × 5 km area, March 18). Ist overlay — Photographic categories, 2nd overlay — SLAR categories (- - - significant ridges, → flight track).*

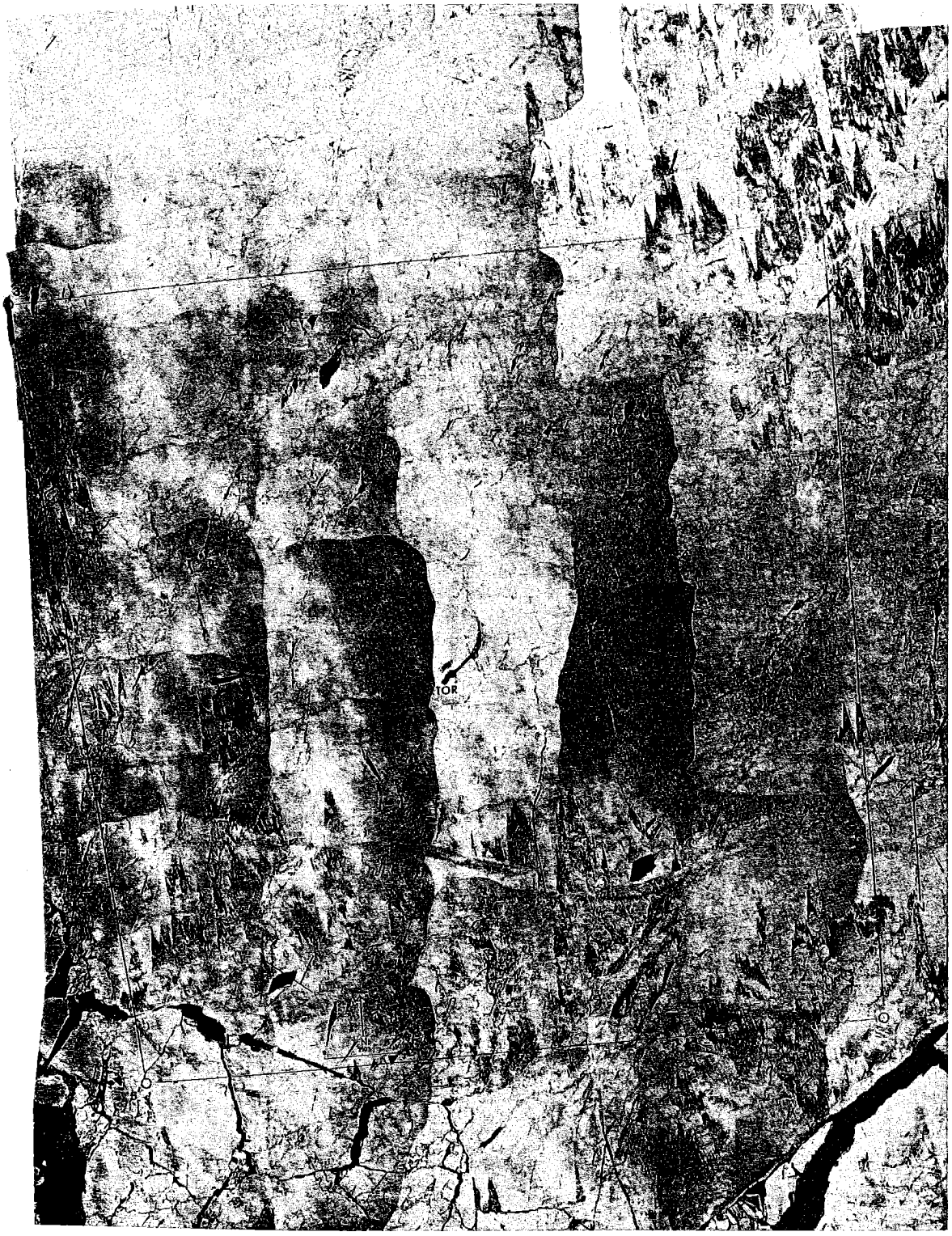

categories thus obtained were termed 'SLAR categories'. Such an overlay with SLAR categories marked on it is shown on top of Figure 10. Essentially, radar imagery exhibits two graytones: bright and black. This overlay was prepared with a purpose to see which photographic categories combine to form the SLAR categories. In retrospect, it was probably unnecessary in the present case to prepare the first overlay, that showing photographic categories, but it does demonstrate the procedure which need and should be followed to conduct a systematic study.

Ice enclosed by the lined areas on the top overlay gives a black tone or no return as is evident on Figure 11. The remaining ice gives a bright tone or a bright return on the radar image. A comparison of the two overlays would show that in most instances the first four photographic categories combine to form the first SLAR category which gives black tone and the remaining four photographic categories combine to form the second SLAR category which gives white tone. So, essentially, only two categories of ice can be identified on the radar imagery: ridges — white, and no ridges — black; or rough and smooth. There are apparently no detrimental masking effect of snow cover, for no difference is evident, on the radar imagery, between snow covered and snow free ice. The SLAR category termed 'no ridges' includes open water and level ice, that is areas which are relatively smooth. Thus, on the basis of gray tone alone it does not seem possible to distinguish ice from no ice or open water on the radar image. This indiscrimination could very well be because of lack of surface details on level ice as a result of improper gain setting or improper choice of imaging angles or both. This result seems to be consistent, though, with past measurements. It was reported by Jirberg and others (15), that open water areas can not be distinguished from level ice simply on the basis of gray tone; both appear black on the radar imagery. This observation was made on X-band radar images of lake ice obtained over the Great Lakes area, though, the imaging angles were not reported (15). The ice in the Great Lakes region should be quite similar to very low salinity ice found during this experiment. It is possible to locate, distinguish, and discriminate open water areas on the basis of surroundings, shape, size, and sharpness of edges and roundness of corners.

The SLAR category termed 'ridges' includes ridges, leads with ice/water edges, fractures, tracks, and very rough ice. The bright return given by these categories is again consistent with radar measurements over lake ice reported by Jirberg and others (15).

Even though there is no gray tone variation on the radar imagery, a comparison of Figure 10 and Figure 11 shows a remarkable correspondence between the radar image and the photo-mosaic. It is possible to identify individual ridges on the radar image and some of these are marked on the overlay on Figure 10. To help make a comparison, some corresponding features are identified on Figures 10 and 11. Floes of level ice as small as 100 meters can be identified on radar imagery.

Some of the features which appear bright on the radar imagery are not readily visible on the photo-mosaic. Thus, an enlarged view of the ice enclosed in the small box around 'TOR' on Figure 11 is shown in Figure 12. The corresponding area on the mosaic is shown in Figure 13 with an enlarged overlay giving the SLAR categories. Some of the areas which show up as bright on the radar image can be easily identified on the enlarged portion of the mosaic and on the corresponding individual photos when viewed through the light table. Some of the areas on the mosaic which you would think give a bright return on the radar image, in fact do not. 'TOR' can be readily identified along with its track through the ice. The direction, location, and width of individual ridges, cracks, and narrow leads can be ascertained. It does not seem possible to infer the height of individual ridges from the radar image. Nor can ridges be separated from ice/water edges of small leads on the basis of tone alone. The radar image shown in Figures 11 and 12 is a reproduction of the line going east to west about 2.4 n.m. south of 'TOR' on flight 953.

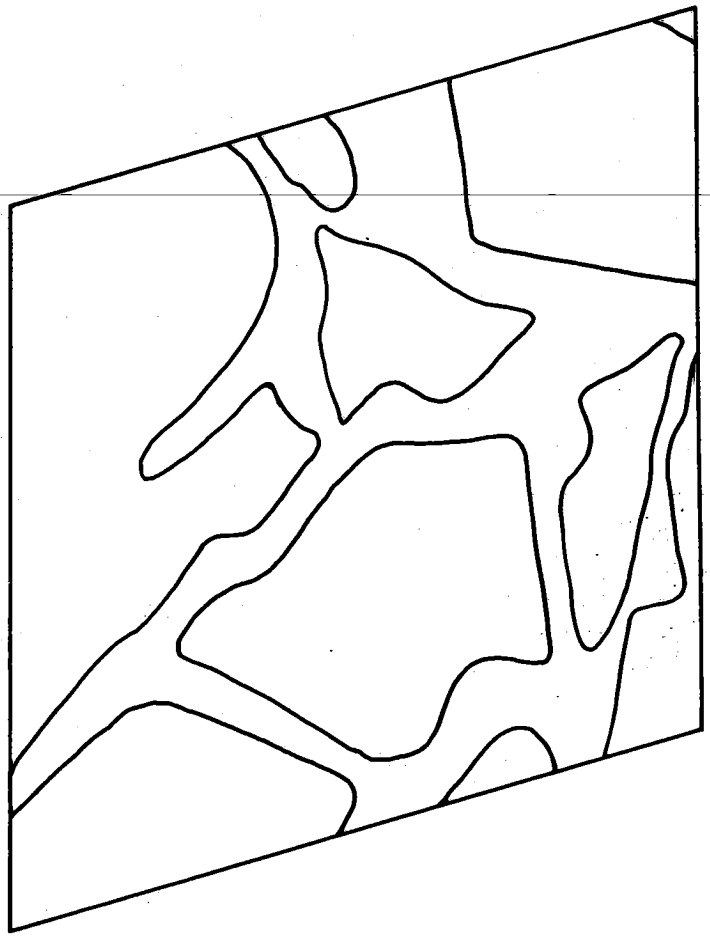

To demonstrate the consistency of radar data, Figure 14 shows a section of the radar imagery obtained during flight number 951 of line going east to west about 2.4 n.m. south of 'TOR'. The mosaic of 5 × 5 km region for the corresponding area with a lay-over showing the SLAR categories is presented in Figure 15. Some of the features are identified on both the mosaic and the radar image to help make the correspondence between the two. There appears to be a system malfunction on the top right hand side of the radar image. It is readily apparent when Figures 11 and 14 are compared. A comparison of these two figures also shows the consistency of radar in mapping the same features. Again only two categories can be identified on the radar image of Figure 14: ridges and no ridges. Enclosed areas on the lay-over of Figure 15 appear white and the open areas white. Individual ridges can be identified and are marked on the overlay. The overall tone of the image is less bright than the one in Figure 11, probably because of the range and gain setting.

Figure 14. *Radar image (5 × 5 km area, Flight 951).*

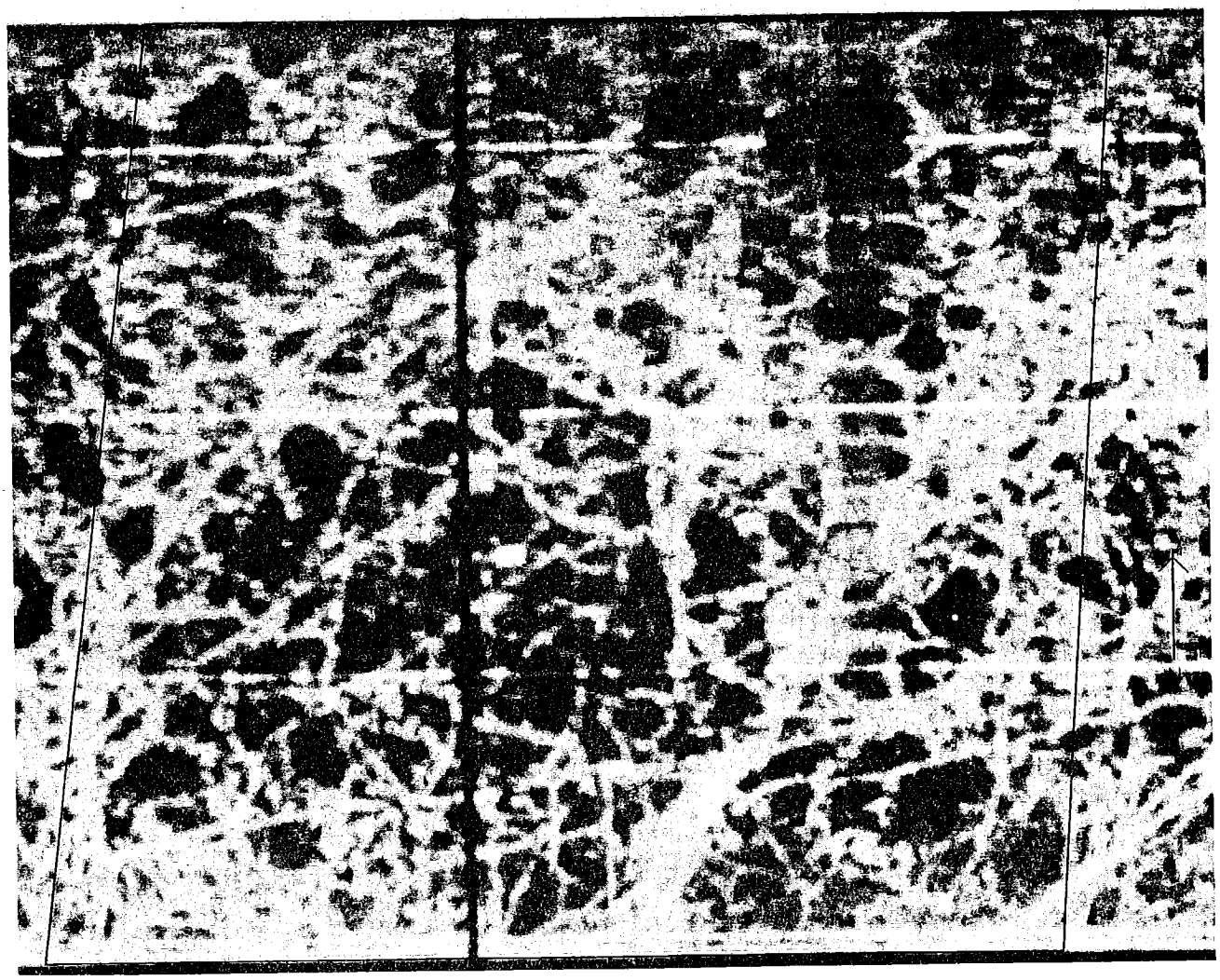

The radar image of the larger 15 × 15 km area is shown in Figure 16. This image is a reproduction of one run over 'TOR' of flight number 952. The air-photo mosaic of the corresponding area is shown in Figure 17 with a overlay giving the SLAR categories. The scale on the mosaic is about twice of that on Figures 11 and 15. Again the white tone on the radar image is because of ridges corresponding to the open ice areas on the mosaic and overlay. Black tone is due to relatively smooth areas or 'no ridges' as given by enclosed areas on and the overlay and mosaic. The top part of the radar image is enlarged and shown in Figure 18. The photo-mosaic and overlay corresponding to this area are shown in Figure 19. Figure 20 shows an enlarged view of the area enclosed by the marked box on the bottom half of Figure 16. The photo-mosaic and the overlay corresponding to this are shown in Figure 21.

There are no new observations that can be made in these figures except the fact that individual ridges can be identified in comparison with level ice. There are some open water areas in the bottom part of image on

(continued on page 36)

Figure 15. *Photo-mosaic corresponding to Figure 14 with overlay showing SLAR categories (- - - significant ridges, → flight track).*

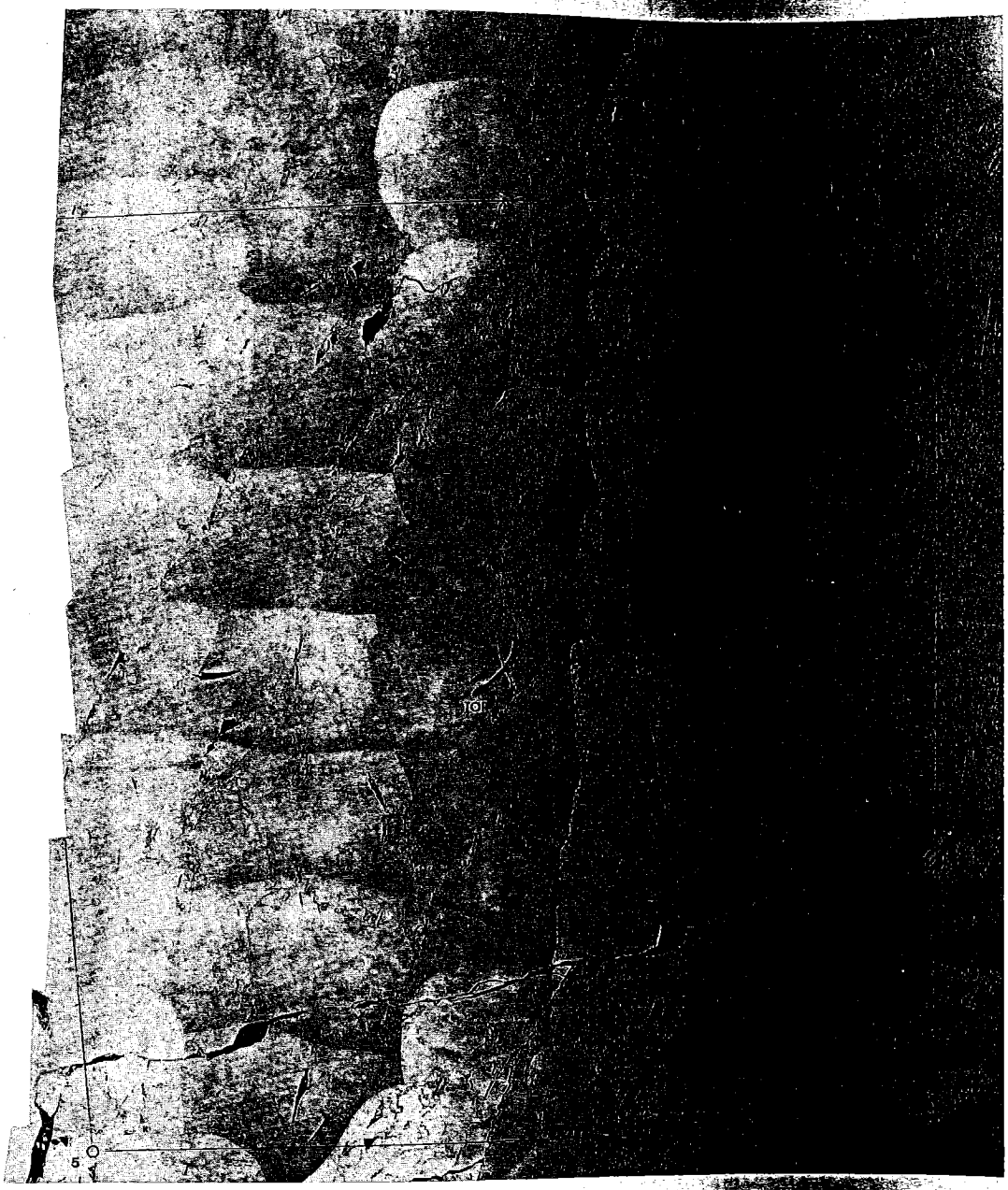

Figure 16. *Radar image (5×5 km area, Flight 952).*

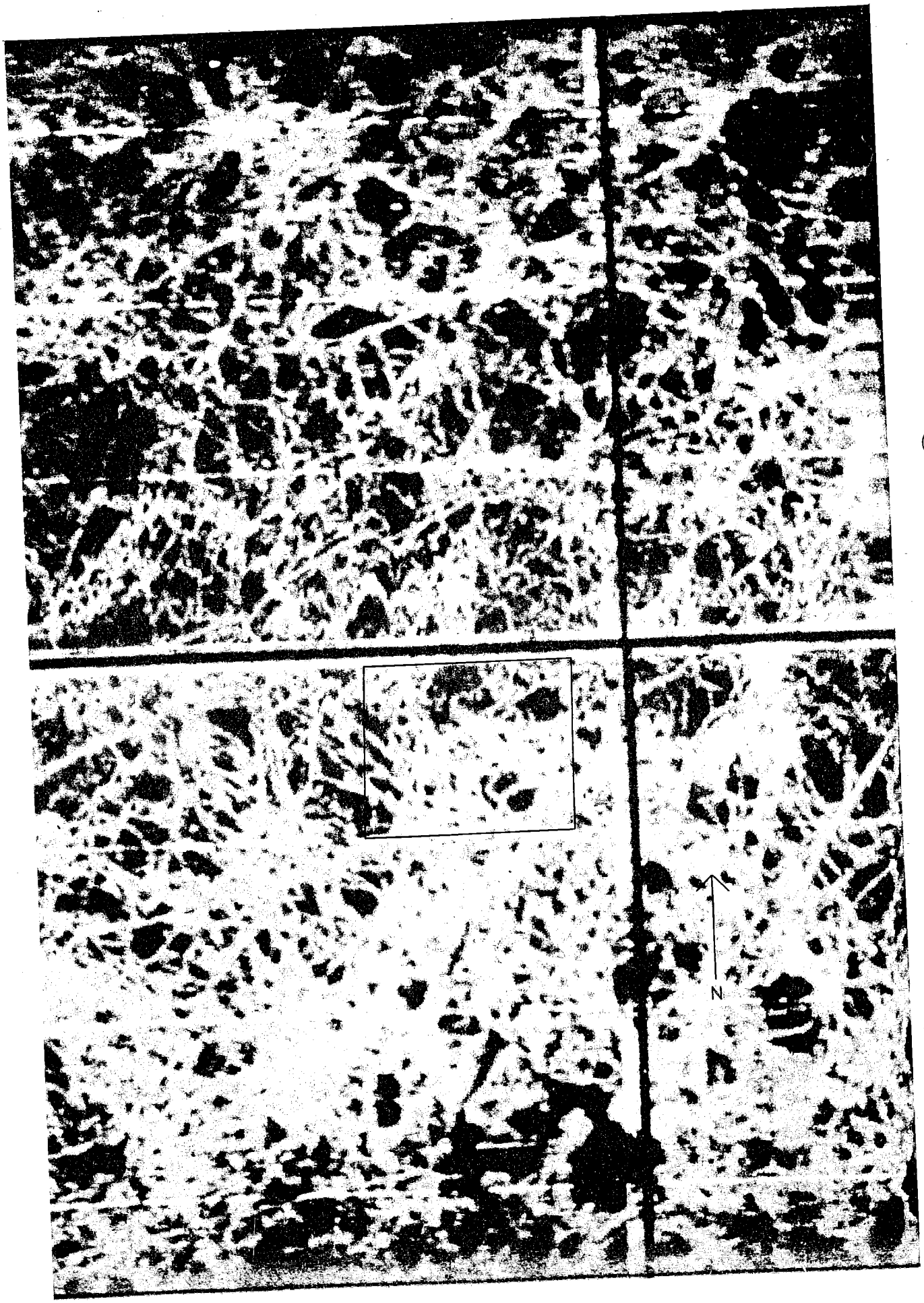

Figure 17. *Photo-mosaic corresponding to Figure 16 with overlay showing SLAR categories (- - - significant ridges, → flight track, ○ radar reflectors visible with SLAR).*

Figure 18. *Radar image, enlarged view of top half of Figure 16.*

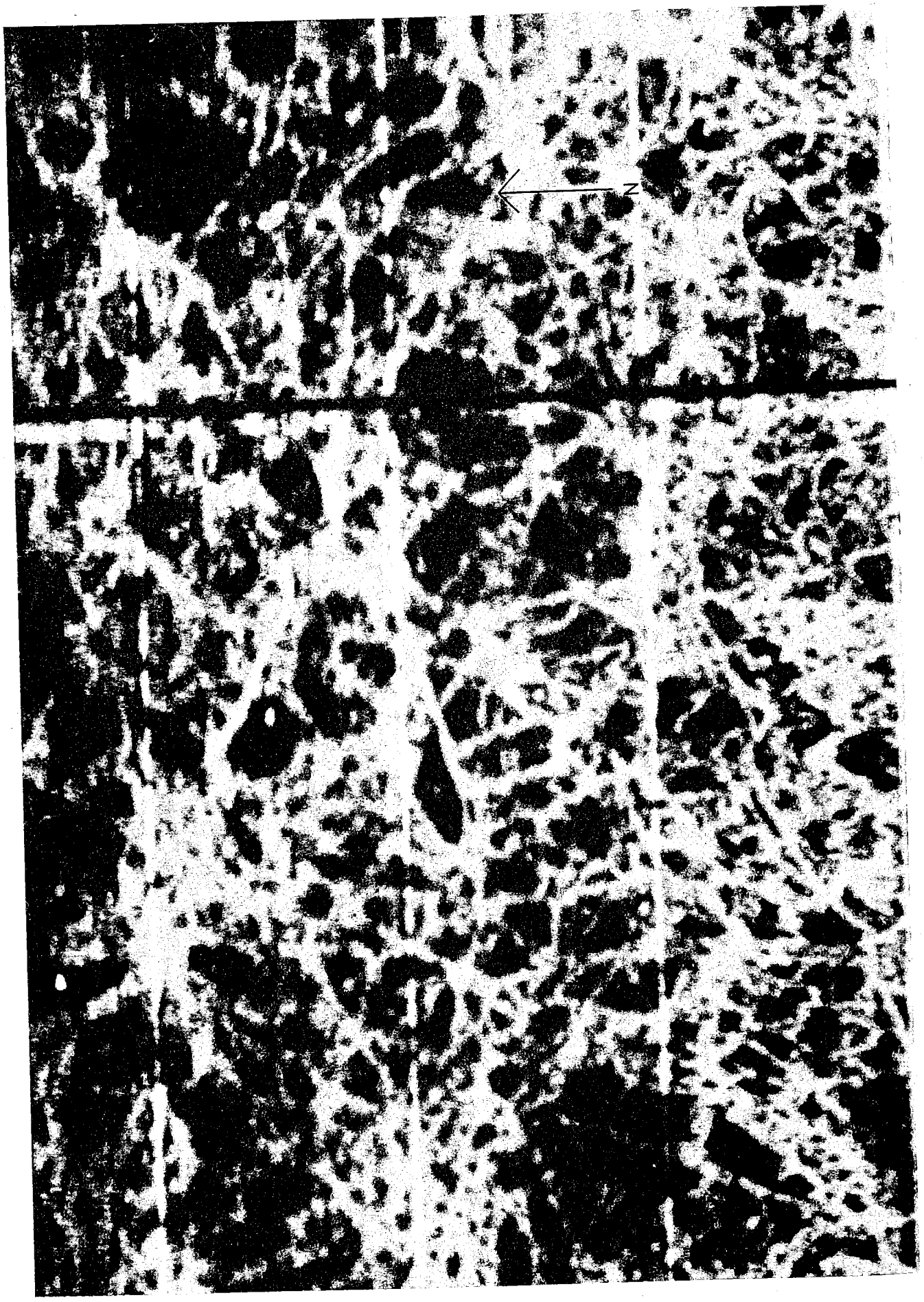

Figure 19. *Photo-mosaic corresponding to Figure 18 with overlay showing SLAR categories.*

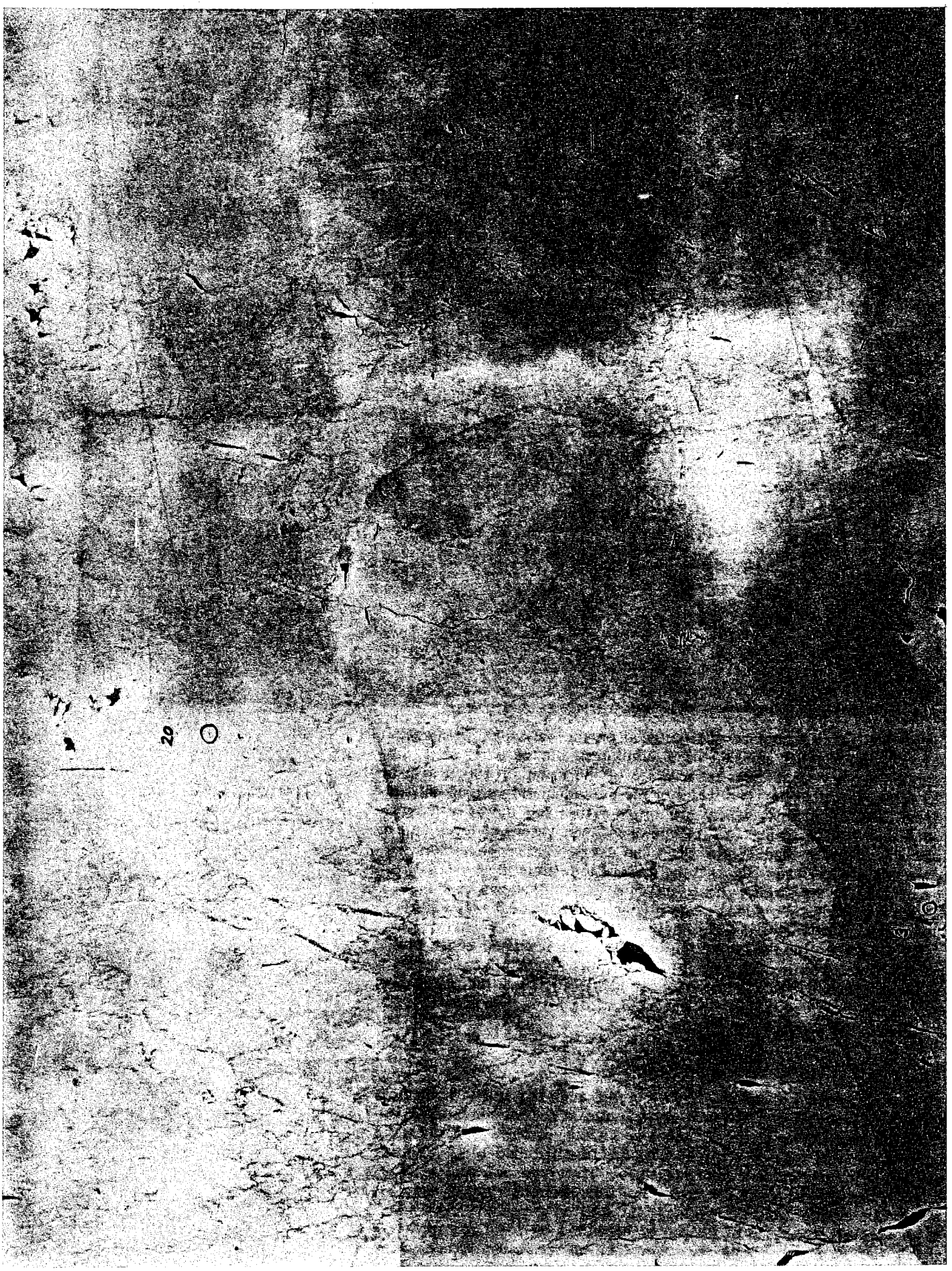

Figure 20. *Radar image, enlarged view of box marked on Figure 16.*

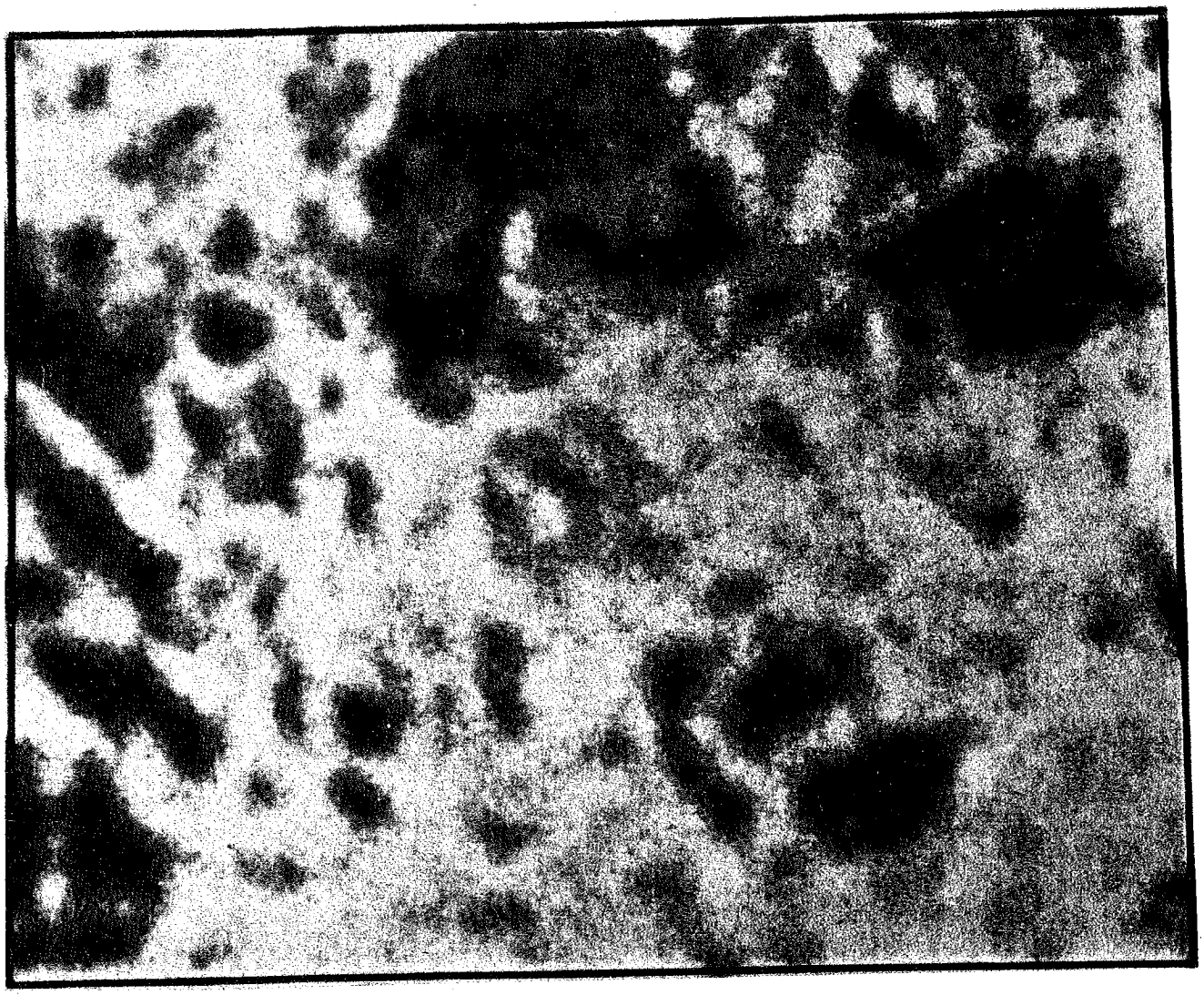

Figure 16, but it cannot be differentiated on the basis of tone alone. It has very sharp edges and can be discriminated on the basis of its surroundings. Very small floes of level ice of the order of 100 m can be identified. The direction and width of the individual ridges is readily apparent. The large areas which give bright return are the areas of very rough, heavily ridged ice. In this type of ice, small floes of level ice can sometimes be identified. Again ridges can not be distinguished from narrow leads and ice/water edges on the basis of tone alone.

The relative appearance of ice and open water is shown in Figure 8. On the basis of observations made in Figures 10 through 21, Figures 4 through 8 can be analyzed accordingly.

The bright returned areas are the ridges, cracks, ice/water edges, faults, and fractures. The heavily ridged ice also gives bright return. The areas of low return or black tone are the level ice. In Figure 8, the open water area is distinguished simply on the basis of its location and size. Open water with slush is shown in Figure 7.

7.2 Discussion of results and conclusions

As is evident from above the quality of the analyzed SLAR imagery is from poor to moderate. There is no variation in the graytone. Only two extreme tones can be identified: black and white. In between gray shades are absent. This lack of graytone variation is attributed to gain setting and/or improper choice of imaging angles. The over- and under- saturation evident in the images is because of operational setting of radar. It can not be attributed to the photographic film or processing. As a result of above, only two types of ice can be identified on radar imagery. One giving high return and, thus, the bright tone on the image. Other, giving no return, and thus appearing black. On the basis of comparisons made with the photo-mosaic, the first type of ice includes ridges, ice/water ed-

Figure 21. *Photo-mosaic corresponding to Figure 20 with overlay showing SLAR categories.*

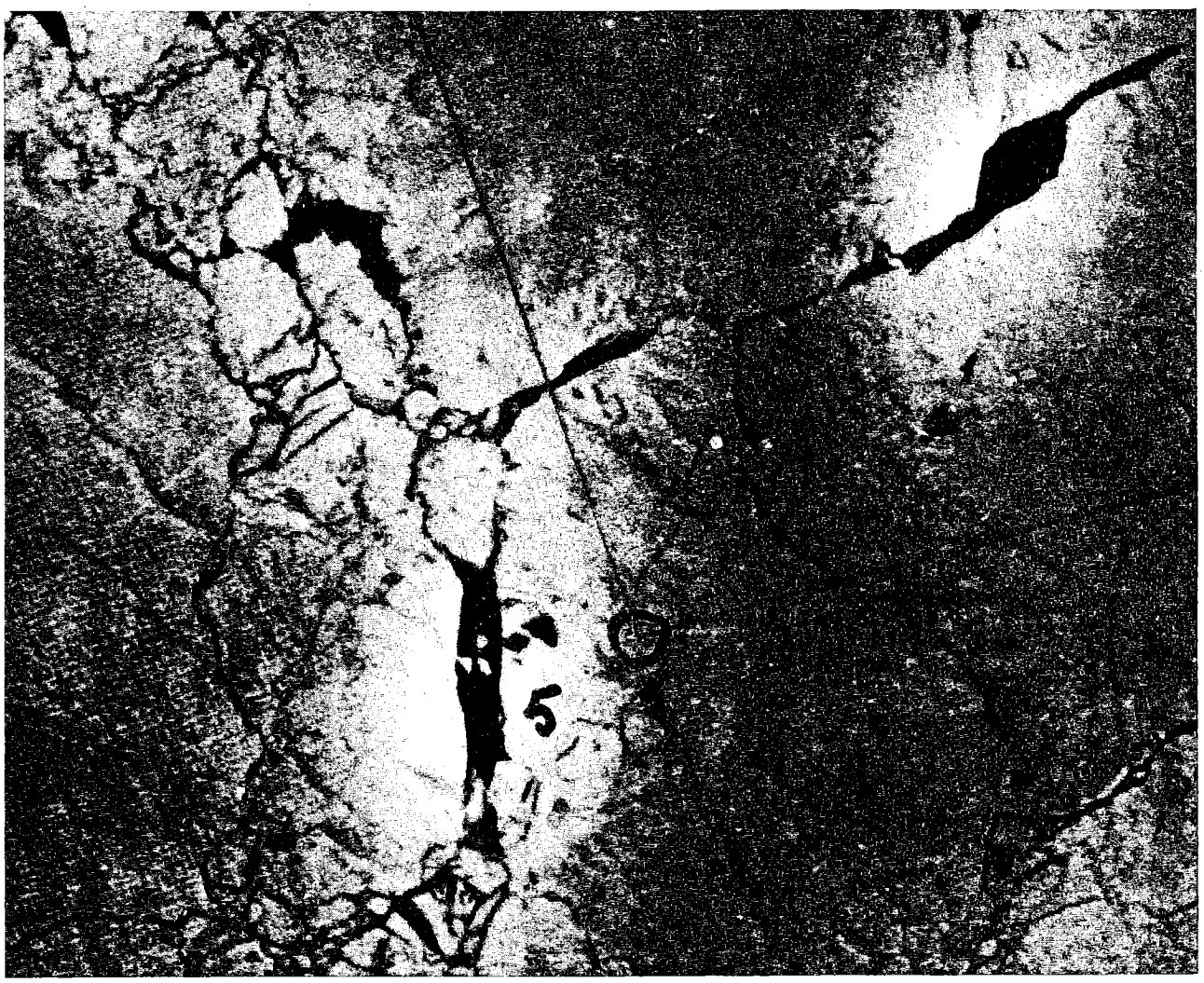

ges, narrow leads covered with broken ice pieces, fractures, cracks, finger raftings, faults, and very rough surfaces. The second type includes level ice with a relatively smooth surface and open water areas. Individual ridges can be identified along with small floes of level ice. Open water areas can not be distinguished from level ice on the basis of tone alone. Individual ridges can not be separated from cracks, ice/water edges, and leads on the basis of graytone alone.

The results obtained here are consistent with the results obtained in the past from radar measurements over lake ice in the Great Lakes region (15) in terms of level ice and water giving no return and brash ice giving bright return.

Despite not so good quality of the radar images presented here, the utility of SLAR can still be appraised for navigational purposes. Shipping routes can be selected through areas which appear black and along the edges of bright areas. The idea is to avoid navigation through white areas which have considerable spatial extent. Routes can be selected along individual ridges which are not easy to navigate through.

For climatological and meteorological models, one measure of roughness can very well be the percentage of ice area giving bright return in the appropriate grid size. Ice and no-ice can be located on the basis of size, shape, and surroundings. Since individual ridges can be separated from very rough ice on the basis of spatial extent, thus, essentially for practical purposes three types of ice can be identified on the radar imagery: ridges, level ice, and very rough ice. There appears no detrimental effect of snow cover. Snow in the present instance does not seem to mask the ice signature. A measure of relative ice drift can be obtained from comparing images obtained on two different days.

8 Recommendations

On the basis of results presented above and the past radar measurements over ice, a number of recommedations can be made for the design of future ice mapping experiments and for the desirable parameters of an operational ice surveillance system.

'Sea Ice -75' experiment was probably well planned with a collection of good ground truth gathering system, but in the end like any other experiment it failed to achieve some of its objectives. This is quite evident in relation to SLAR measurements. The failure to meet the objectives is partly because of the performance of SLAR and partly because of the design of experiment itself. Radar imagery from parallel flight lines which was supposed to overlap, in fact does not. Photo-mosaics of larger 15×15 km area on two days (March 13 and 18) are not available. Mosaics of this area are only available for the March 14 flight. It is very difficult to correlate radar imagery obtained on the 18th with the mosaic of the larger area obtained on the 17th. As a result of this, substantial amount of radar imagery is without the support of corresponding photo-mosaics and subsequent ground truth. The flights which were made over 'TOR' do not cover any area on the 5×5 km mosaic. Only one flight line was made on the 14th and that too over 'TOR'. As a result most of the 15×15 km is not mapped for which a photo-mosaic is available.

It seems that 5×5 km area is in fact too small to contain any repetative features of variety. It is too small for establishing general ice conditions and ascertaining ice trends. Only a measure of relative ice drift is obtainable. The ice drift is not readily evident because of small area. No fixed reference point is available for measuring absolute drift.

The quality of radar imagery obtained could certainly be better. Graytone resolution is lacking on the radar image. The features which show up on the radar image are probably the ones which can be readily identified on the image obtained under poor operating conditions. Even then a substantial amount of ice information can be obtained through these images. In addition to the various ice features, radar reflectors can be readily identified when located in the areas of level ice. The images obtained are not sharp. They have a hazy and blurred appearance similar to the one given by an out of focus object in a photographic process. It could be because of the range setting or the photographic process itself. The spatial resolution cell size seems to be adequate enough for mapping ice for both navigational and climatological forecasting.

The need to conduct a well designed experiment with a properly operated SLAR is readily apparent from above. A need exists to ascertain the effect temperature might have on the ice signature. The masking effect of snow cover, if any, is not yet conclusive. It is not yet clear whether open water can be distinguished from level ice or ice ridges from ice/water edges on the basis of tone alone or relative contrast. It is not conclusive if diffferent types of level ice can be discriminated thereby providing information of relative ice thickness. There exists a need to find optimum operation radar parameters such as angles, polarizations, and frequencies, along with the necessary and sufficient repetative timely coverage.

The following recommedations for the design of future experiments are made keeping in mind the results obtained from this and past radar ice measurements:

A. Experimental Area

1. The entire experimental area should be at least 30×30 km. It should be well defined and marked by latitudes and longitudes. It should contain various types of ice categories and features such as ridges, cracks, leads, different types of level and rough ice. Large and small areas of open water should be present so that the ability of SLAR

to distinguish open water from level ice and ice ridges from ice/water edges can be ascertained.

Such an area would be large enough to contain enough repetative features and to provide measure of absolute ice drift.

2. A smaller area about 10×10 km should be marked within the larger area with radar reflectors. This would provide the indication as to the movement of smaller ice area in relation to the fixed larger area defined by latitudes and longitudes.

B. Ground Truth Information

1. Ground truth information should only be obtained for small areas representative of various ice types and features. It is not desirable to cover 1×1 km area extensively in detail as was done in this experiment. Rather, what is needed is to gather ground truth information for areas large enough to be identified on the aerial photographs and radar imagary. These very small areas representing one specific experimental area. In addition spot measurements should also be made. The following measurements should be made:

   I) Salinity: It is important, but not very, in view of the presence of low salinity. Both the surface salinity and the salinity profile should be ascertained. It would be helpful to know the variations of salinity in the horizontal direction.

   II) Ice thickness: Ice thickness measurements should be made for various ice types and features.

   III) Temperature: Surface temperature and the temperature profile measurements should be made.

   IV) Snow Cover: Snow thickness if it is present along with the surface conditions, whether wet or dry, should be ascertained.

   V) Surface roughness: A measure of quantitative and relative surface roughness should be made. It would be helpful to ascertain the surface height profile for few representative areas.

   VI) Height and spatial extent of individual ridges and ice/water edges should be made.
2. Photo-mosaics corresponding to the entire experimental area at the scale of at least 1:10,000 should be made available. These mosaics would primarily act as ground truth information.

C. Mapping Considerations

1. Mapping of the entire 30×30 km area should be accomplished.
2. In mapping, a fixed reference point should be established.
3. Same area should be mapped at different altitudes to ascertain the effect of altitude. It would be highly advantageous to map the same area at scales of 1:50,000, 1:100,000 and 1:200,000 to find the optimum scale of presentation. A scale which is useful for providing information for climatological model may not be so for navigational purposes.
4. Mapping of the same area, under similar operating conditions, should be done for various temperature conditions, so that the effect of temperature can be ascertained.
5. Mapping should be done both before and after the snow fall, so as to ascertain masking effect of snow cover.
6. Same area should be mapped at various imaging angles, to find optimum angles of operation.
7. It would be helpful to map the same area on successive days to see the changes in conditions, drift, and growth pattern of ice cover. It would also show the opening and closing of narrow leads and build of pressure ridges.

   It would be desirable to have fresh ice breaker tracks in the area. It would be useful to see if the growth of ice in the track is different from that in other leads and if it can be identified. What is actually needed is to map the same area in the successive stages of its growth.
8. An operational ice surveillance system would in fact provide repetative and timely coverage over the same area. So, essentially, SLAR data would be available over repeated time frame. Thus, the SLAR imagery analysis need not be based only on the current or latest piece of imagery. It should be based on the past growth history of ice and the past sequential pieces of imagery. So, the features which can not readily be identified and discriminated on a single current or latest

piece of image could very well be identified when the images from the previous days are taken into account. This holds true for such features as ice thickness, pressure ridges, leads, ice/water edges, and so on. The idea of change detection has to be incorporated into the imagery interpretation procedure, that is, to be able to detect changes in the latest piece of radar imagery in relation to past measurements. The idea is to detect and identify those features which actually change with time such as opening and closing of leads, formation of ridges etc., and others which do not like level ice areas. How well past images would help in the analysis and interpretation of the latest piece of image, need to be established by an experiment. The adequate and necessary repetative coverage required to make the past images useful in the interpretative process has to be ascertained. The conditions under which a more frequent coverage would be necessary need to be identified. It would also be desirable to ascertain the size of the area which need to be mapped depending on the rate and the direction of drift and the changes in temperature.

The utility of radar in mapping ice must not only be based on one piece of imagery. Rather it should be based on information available from images obtained over a number of days. It is precisely for this reason that the repetative and timely coverage provided by a radar is seen to be attractive for ice surveillance. So, what desirable is to conduct an experiment which would help study and demonstrate this quality of SLAR imagery. The concept of use of radar is not only for ice mapping, rather it is for ice monitoring.

D. General Consideration

1. The experiment should also be conducted in such a way which would allow the testing of ice forecasting model on the basis of radar imagery.
2. It must be pointed out that SLAR employed in the experiment should have the appropriate dynamic range and graytone resolution. The proper and optimum operation of the SLAR must be ensured.
3. It would be desirable, though difficult and expensive, to map the same area by SLAR's operating at a higher and a lower frequency band and having different resolution cell sizes. It would be highly advantageous to have a cross-polarized image (Horizontal transmit — Vertical receive or Vertical transmit — Horizontal receive), in addition to like-polarized (Horizontal — Horizontal or Vertical — Vertical) image, of the same area made available.

Because of a lack of enough available information, it is quite difficult at present to specify optimum parameters and characteristics for an operational ice surveillance SLAR. This should be a basis for a larger study and be conducted after or in conjunction with the above mentioned experiment. In the meantime some desirable characteristics of a prototype system can be listed below:

1. X-band, about 3 cm wevelength.
2. VV or HH polarization, there does not seem to be any difference at present. Provision should be made to add VH or HV capability later.
3. 0,1 to 0,2 μspec pulse length so that a range resolution of 30 meters can be achieved.
4. Antenna beamwidth of less than or equal to 0,5 degrees so that an azimuth resolution of at least 8 R_{km} in meters can be achieved (R is the range in km).
5. A swath width of at least 15 km and preferably 20 km.
6. A variable antenna so that imaging angles from 10 to 90 degrees can be obtained.
7. Provision to obtain various scales, 1:50,000, 1:100,000, and 1:200,000. A scale of 1:50,000 should be good enough for navigational purposes. A scale of 1:100,000 may be desirable for ice forecasting.
8. Data must be presented on a photographic film along with digital tape.
9. A graytone resolution corresponding to a resolution of 0,5 dB in σ°.
10. Antenna should be compensated for range, cosec^2.
11. True ground range presentation.
12. A dynamic range of 60 dB with a minimum value of σ° detectable to about —45 dB at about 85°.
13. Almost a square resolution cell at mid ranges, so that images obtained from perpendicular flights can be readily compared.

14. Variable gain setting and automatic gain control.
15. Aircraft should be quite stable so as not to provide image distortions.
16. The number of independent cells should be about 100, this of course will depend on the angle and the size of the resolution cell. There is a trade-off between the graytone resolution and spatial resolutions pointed out by Moore (32). This should be further studied. Mode rate spatial resolution is acceptable as long as significant graytone resolution is obtained. The trade-off should be in the direction of better graytone resolution.

At present there is no need to have the images relayed in the real time to the ice-breaker and ships for route selection. This can be achieved by processing the data on the ground and relaying the necessary information from there. The actual operational system will certainly have the capability to automatically process the data or images and relay them directly to ice-breakers and ships for navigational purposes. Even for designing a proto-type system, it would be useful to conduct a short study to establish its desirable characteristics and provide cost/benefit analysis.

The rate and the amount of data gathered by an operational system would be tremendous. Such a large quantity of data can only be handled through semi-automatic means, that is, largely automatic processing done under marginal human supervision and control. It is for this reason that the utility of automatic processing techniques such as pattern recognition should be explored. The quality of images obtained from "Sea Ice -75" is not good enough to test such techniques. It is recommended to conduct studies with a view to automatically process and classify data collected from future erperiments.

To design an optimum operational ice imaging radar of general utility, it is important to know the effect of frequency, angle, polarization, and resolution in discriminating ice. It is impossible to make experimental measurements corresponding to different parameters. That is why it would be desirable to have a theoretical model which can predict the radar scattering from sea ice. Such a model can be tested under controlled experimental conditions, which would require measurements of electrical properties of ice.

This model would not only be useful in understanding the nature of radar return from sea ice but it would also help in the analysis of SLAR data and in specifying operational parameters of radar. It is recommended that such an analytical study be conducted along with its proper testing.

The operating parameters for an operational ice surveillance system should be based on results presented here, results obtained from future experiments, and theoretical studies.

9 Summary of Results

The results from "Sea Ice -75" experiment indicate that despite the poor quality of radar images, three categories of ice can be identified: ridges, no ridges, and very rough ice broken. So, essentially, only ridges, ice/water edges, fractures and leads, and very rough ice is mapped which gives a bright return. The use of near grazing angles which were employed here is probably only good for mapping these features. The areas of level ice and open water give no return and hence appear black on the image. Probably because of improper setting of gain and/or improper use of imaging angles which has resulted in over-or under-saturation, the surface details on the level ice are lacking. This does not make it possible to discriminate level ice from open water on the basis of tone alone. Open water area, can be differentiated, however, on the basis of sharpness of edges, and its size and location. In view of the objectives of this experiment, the following results can be specifically stated:

1. Ice can not be differentiated from non-ice on the basis of tone alone. However, non-ice areas can be identified on the basis of location.
2. Ice concentration can be measured only when open water areas are separated from level ice.
3. A measure of roughness of ice can be only obtained in spatial context. The relative vertical distribution or variation of surface profile are not evident because of lack of graytone variation.
4. Level ice can be distinguished from rough ice when it can be separated from open water areas. Radar images can never give a measure of ice thickness directly. It can help divide ice into categories. For this purpose, enough surface details and texture have to be present to provide a measure of relative thickness.
5. The state of ice can not be ascertained because of lack of graytone variation and thereby the texture. There appears no detrimental effect of snow cover.
6. What the radar sees is ice edges, especially at these angles. Ice ridges can not be separated from ice/water edges on the basis of tone alone.

It must be pointed out that because of not so good quality of radar images the results and observations presented above are by no means conclusive. It is quite clear that at worst radar images can provide at least information about ridges, level ice or open water, and moderate to heavy rough ice. The results presented here are consistent and in agreement with past radar measurements over lake ice (32), yet by no means are conclusive. The utility of a radar imager for operational ice surveillance must not be solely based on the results presented here. Rather, the ability of radar to provide repeated and timely coverage must be kept in mind. The allweather, day/night operational capability of radar to provide a broad areal coverage is very useful. This along with its ability to achieve good spatial and graytone resolution, both from aircraft and spacecraft altitudes, are greatest assests of radar imager.

10 Conclusions

A review of the above would indicate that SLAR (Side-Looking Airborne Radar) has enough proven and demonstrated necessary capabilities to be the primary remote sensor in future operational ice surveillance system. It should be pointed out that orbiting satellites will be used in the future to act as platforms for the remote sensors, for the need to map large areas. The **same resolution** can be obtained from the satellite and aircraft altitudes by a SLAR system.

It would be highly desirable to study the ability of other remote sensors such as microwave radiometer and IR thermal scanner to aid and support the ice information gathered by SLAR. The data obtained by these sensors can help interpret and calibrate the SLAR images. These sensors can, thus, act as secondary sensors in the over all ice information gathering systems.

The ice conditions found in the Bothnia (both Bay and Sea) are quite different from those found in the Arctic. Thus, the capabilities and limitations of any remote sensor must not be solely based on its performance in the Arctic. Therefore, a need exists to conduct further remote sensing experiments in the Bothnia itself so that various sensors can be tested adequately. The ice conditions prevalent in the Bay of Bothnia are similar to those found in the Great Lake region of Canada. But the conditions found in the Sea of Bothnia are closer to those found in the Arctic because of the presence of higher salinity. The temperatures prevalent in the Bay and Sea of Bothnia the winter 1975 were about 4 to 5°C above normal. Whether the results presented here would be equally valid under other temperature conditions must await future experimental results.

References

1. Fletcher, J.O., "Probing Secrets of Arctic Ice", AIDJEX Bulletins.
2. Anderson, V.H., "High Altitude, Side Looking Radar Images of Sea Ice in the Arctic", Proceedings Fourth Symposium on Remote Sensing of Environment, University of Michigan, Ann Arbor, Michigan, USA, pp. 845—857, June, 1966.
3. Johnson, J.D. and L.D. Farmer, "Use of Side-Looking Airborne Radar for Sea Ice Identification", Journal of Geophysical Research, Vol. 76, no. 9 pp. 2138—2155, March 1971.
4. Johnson, J.D. and L.D. Farmer, "Determination of Sea Ice Drift Using Side-Looking Airborne Radar", Proceedings 7th International Symposium on Remote Sensing of Environment, The University of Michigan, Ann Arbor, Michigan, USA, May, 1975.
5. United States Coast Guard, "Data Reduction of Airborne Sensor Records", Report No. DOT-CG-01-800-A, Department of Transportation, Office of Research and Development, Washington, D.C. 20591, USA, July, 1970.
6. United States Coast Guard, "Analysis of SLAR Imagery of Arctic and Lake Ice", Report No. DOT-CG-14486-A, Department of Transportation, Office of Research and Development, Washington, D.C. 20591, March, 1972.
7. United States Coast Guard, "Interpretation of Winter Ice Conditions from SLAR imagery", Report No. DOT-CG-14486-1A, Department of Transportation, Office of Research and Development, Washington, D.C. 20591, February, 1972.
8. Glushkov, V.M. and V.B. Komarov, "Side-Looking Imaging Radar System TOROS and Its application to the Study of Ice conditions and Geological Explorations", Proceeding 7th International Symposium on Remote Sensing of Environment, University of Michigan, Ann Arbor, Michigan, 1971.
9. Loshchilov, V.S. and V.A. Voyevodin, "Determination of Elements of Ice Cap Drift and Movements of Ice Edges by Means of the Airborne Side-Scan Radar 'TOROS'", Problems in Arctic and Antarctica, Vol. 40, pp. 23—30, 1972.
10. Ketchum, R.D., Jr. and S.J. Tooma, Jr., "Analysis and Interpretation of Airborne Multi-Frequency Side-Looking Radar Sea Ice Imagery", Journal of Geophysical Research, Vol. 78, no. 7, pp. 520—538, 1973.
11. Rouse, J.W. Jr. "Arctic Ice Type Indification by radar", University of Kansas Center for Research, Inc., CRES Technical Report 121—1, Remote Sensing Laboratory, Lawrence, Kansas, USA, August, 1968.
12. Parashar, S.K., et.al., "Investigation of Radar Discrimination of Sea Ice", Proceedings 9th International Symposium and Remote Sensing of Environment, University of Michigan, Ann Arbor, Michigan, 1974.
13. Parashar, S.K., "Investigation of Radar Discrimination of Sea Ice", (Ph. D. Thesis), University of Kansas Center for Research, Inc., CRES Technical Report 185—13, Remote Sensing Laboratory, Lawrence, Kansas, USA, 1974.
14. Parashar, S.K., et.al., "A Theory of Wave Scatter from an Inhomogeneous Medium with a slightly Rough Boundary and its Applications to Sea Ice", Proceedings URSI Specialist Meeting on Microwave Scattering and Emission from the Earth, Berne, Switzerland, September, 1974.
15. Jirberg, R.J., et.al., "Application of SLAR for Monitoring Great Lakes Total Ice Cover", NASA TMX-71473, NASA Lewis Research Center, Cleveland, Ohio, 44135, USA, December, 1973.
16. Larrowe, B.T., et.al., "Fine-Resolution Radar Investigation of Great Lakes Ice Cover", Final Report, Willow Run Laboratories, University of Michigan, Ann Arbor, Michigan, Jan., 1971.

17. Groen, P., The Waters of the Sea, D.Van Nostand Co. ltd., London, 1967.
18. Weeks, W.F. and A. Assur, "Fracture of Lake and Sea Ice", Research Report 269, Cold Regions Research and Engineering Laboratory, Hanover, New Hampshire, USA, September, 1969.
19. Dunbar, M., "A Glossary of Ice Terms (WMO Terminology)", Ice Seminar, Special Volume 10, The Canadian Institute of Mining and Metallurgy, pp. 105—110, 1969.
20. Weeks, W.F., "Understanding the Variations of the Physical Properties of Sea Ice", Special Report 112, Cold Regions Research and Engineering Laboratory (CRREL), Hanover, New Hampshire, May, 1967.
21. Assur, A., "Composition of Sea Ice and Its Tensile Strength", in Arctic Sea Ice, U.S. National Academy of Sciences, National Research Council, Publication 598, pp. 106—138, 1958.
22. Evans, S., "Dielectric Properties of Ice and Snow — A Review", Journal of Glaciology, Vol. 5, pp. 773—792, 1965.
23. Hoekstra, P. and P. Cappillino, "Dielectric Properties of Sea Ice and Sodium Chloride Ice at UHF and Micro-Wave Frequencies", Journal of Geophysical Research, Vol. 76, no. 20, pp. 4922—4931, July 1971.
24. Skolnik, M.I., Radar Handbook, Mc Graw-Hill Book Company, 1970.
25. Brown, W.M., and L.J. Porcello, "An Introduction to Synthetic-Aperture Radar", IEEE Spectrum, Vol. 6, pp. 523—561, 1971.
26. Blomquist, Å., C. Pilo and T. Thompson, "Sea Ice -75: Programme", Winter Navigation Research Board, Report No 16:1, Norrköping, Sweden, 1976.
27. Swedish Space Corporation, "Registrations Made During "Sea Ice -75", Tritonvägen 27, S-171 54 Solna, Sweden, April 18, 1975.
28. Udin, I and A. Omstedt, "Sea Ice -75: Dynamical Report", Winter Navigation Research Board, Report No 16:8, Norrköping, Sweden, 1976.
29. Udin, I. "Sea Ice -75: Ground Truth Report", Winter Navigation Research Board, Report No 16:2, Norrköping, Sweden, 1976.
30. Morra, R.H.J. and G.P. de Loor, Sea Ice -75: Ice Detection by SLAR, Winter Navigation Research Board, Norrköping, Sweden 1976.
31. Rymdbolaget, "SLAR-registreringar", April 9, 1975.
32. Moore, R.K., "Imaging Radars for Geoscience Use", IEEE Transactions on Geoscience Electronics, Vol. GE-9, pp. 155—164, 1971.

SWEDISH/FINNISH WINTER NAVIGATION RESEARCH BOARD

REPORTS

No. Titel

1. HAVSISKONFERENS. Protokoll (1972).
2. VINTERSJÖFART I BOTTENHAVET — Erfarenheter av SCA:s distributionssystem — L. Sjöstedt och S. Hammarsten (1972).
3. ISSKADOR PÅ FARTYG I ÖSTERSJÖN, BOTTENHAVET OCH BOTTENVIKEN. — Statistisk analys av skadefrekvenser — L. Sjöstedt och S. Hammarsten (1973).
4. PROPELLERPROBLEM. Propellerverkningsgradens beroende av bladutformningen. H.P. Loid (1973).
5. FARTYGS FRAMDRIVNINGSMOTSTÅND I IS. E. Enkvist (1974).
6. VINTERSJÖFART MED STORA FARTYG I BOTTENVIKEN. (1974).
7. VINTERSJÖFART I BOTTENVIKEN. Symposium Luleå (1974).
8. HAVSISUNDERSÖKNINGEN I BOTTENVIKEN VINTERN 1974. A. Omstedt, T. Thompson och I. Udin (1974).
9. KARTERING AV YTVATTENTEMPERATUREN I VATTNEN RUNT SVERIGE. J-E. Lundqvist, A. Omstedt och I. Udin (1974).
10. EXPERIMENTS ON REMOTE SENSING OF SEA ICE USING A MICROWAVE RADIOMETER. M. Tiuri, M. Hallikainen and K. Kaski (1974).
11. BOTTENVIKENS STÅLFYRAR — HÅLLFASTHETSANALYS OCH FÖRBÄTTRINGSFÖRSLAG. M. Määttänen (1974).
12. FORMATION AND STRUCTURE OF ICE RIDGES IN THE BALTIC. E. Palosuo (1975).
13. CALCULATION OF ICE DRIFT IN THE BOTHNIAN BAY AND THE QUARK. A. Valli and M. Leppäranta (1975).
14. A NARROW BEAM SONAR TO MEASURE THE SUBMARINE PROFILE OF AN ICE RIDGE. E. Palosuo, T. Pousi and M. Luukkala (1976).
15. THE AVERAGE SURFACE TEMPERATURE IN THE AUTUMN AND THE EARLY WINTER ON THE GULF OF BOTHNIA, THE NORTHERN BALTIC SEA AND THE GULF OF FINLAND (1966—1974). H. Grönvall and E. Palosuo (1976).

16:1 SEA ICE -75. Programme. Å. Blomquist, C. Pilo and T. Thompson (1975).

16:2 SEA ICE -75. Ground truth report. I. Udin (1976).

16:3 SEA ICE -75. Ice detection by SLAR. R.H.J. Morra and G.P. de Loor (1976).

16:4 SEA ICE -75. Analysis of SLAR data. S. Parashar (1976).

16:5 SEA ICE -75. FLAR, ODAR, ship's radar. J. Nilsson, T. Hagman and Y. Nilsson (1976).

16:6 SEA ICE -75. IR-scanner results. E. Fagerlund and G. Lundholm (1976).

16:7 SEA ICE -75. Radaraltimeter results. S. Axelsson (1976).

16:8 SEA ICE -75. Dynamical report. I. Udin and A. Omstedt (1976).

16:9 SEA ICE -75. Summary report. Å. Blomquist, C. Pilo and T. Thompson (1976).

SWEDISH/FINNISH WINTER NAVIGATION RESEARCH BOARD

REPORTS

No. Titel

1. HAVSISKONFERENS. Protokoll (1972).
2. VINTERSJÖFART I BOTTENHAVET — Erfarenheter av SCA:s distributionssystem — L. Sjöstedt och S. Hammarsten (1972).
3. ISSKADOR PÅ FARTYG I ÖSTERSJÖN, BOTTENHAVET OCH BOTTENVIKEN. — Statistisk analys av skadefrekvenser — L. Sjöstedt och S. Hammarsten (1973).
4. PROPELLERPROBLEM. Propellerverkningsgradens beroende av bladutformningen. H.P. Loid (1973).
5. FARTYGS FRAMDRIVNINGSMOTSTÅND I IS. E. Enkvist (1974).
6. VINTERSJÖFART MED STORA FARTYG I BOTTENVIKEN. (1974).
7. VINTERSJÖFART I BOTTENVIKEN. Symposium Luleå (1974).
8. HAVSISUNDERSÖKNINGEN I BOTTENVIKEN VINTERN 1974. A. Omstedt, T. Thompson och I. Udin (1974).
9. KARTERING AV YTVATTENTEMPERATUREN I VATTNEN RUNT SVERIGE. J-E. Lundqvist, A. Omstedt och I. Udin (1974).
10. EXPERIMENTS ON REMOTE SENSING OF SEA ICE USING A MICROWAVE RADIOMETER. M. Tiuri, M. Hallikainen and K. Kaski (1974).
11. BOTTENVIKENS STÅLFYRAR — HÅLLFASTHETSANALYS OCH FÖRBÄTTRINGSFÖRSLAG. M. Määttänen (1974).
12. FORMATION AND STRUCTURE OF ICE RIDGES IN THE BALTIC. E. Palosuo (1975).
13. CALCULATION OF ICE DRIFT IN THE BOTHNIAN BAY AND THE QUARK. A. Valli and M. Leppäranta (1975).
14. A NARROW BEAM SONAR TO MEASURE THE SUBMARINE PROFILE OF AN ICE RIDGE. E. Palosuo, T. Pousi and M. Luukkala (1976).
15. THE AVERAGE SURFACE TEMPERATURE IN THE AUTUMN AND THE EARLY WINTER ON THE GULF OF BOTHNIA, THE NORTHERN BALTIC SEA AND THE GULF OF FINLAND (1966—1974). H. Grönvall and E. Palosuo (1976).

16:1 SEA ICE -75. Programme. Å. Blomquist, C. Pilo and T. Thompson (1975).

16:2 SEA ICE -75. Ground truth report. I. Udin (1976).

16:3 SEA ICE -75. Ice detection by SLAR. R.H.J. Morra and G.P. de Loor (1976).

16:4 SEA ICE -75. Analysis of SLAR data. S. Parashar (1976).

16:5 SEA ICE -75. FLAR, ODAR, ship's radar. J. Nilsson, T. Hagman and Y. Nilsson (1976).

16:6 SEA ICE -75. IR-scanner results. E. Fagerlund and G. Lundholm (1976).

16:7 SEA ICE -75. Radaraltimeter results. S. Axelsson (1976).

16:8 SEA ICE -75. Dynamical report. I. Udin and A. Omstedt (1976).

16:9 SEA ICE -75. Summary report. Å. Blomquist, C. Pilo and T. Thompson (1976).